Development of mucoadhesive vaginal films with metronidazole using Poly(2-ethyl-2-oxazoline) – Polycarbophil blends via hot melt extrusion

European Polymer Journal 237 (2025) 114175

Contents lists available at ScienceDirect

European Polymer Journal

journal homepage: www.elsevier.com/locate/europolj

Development of mucoadhesive vaginal films with metronidazole using Poly (2-ethyl-2-oxazoline) – Polycarbophil blends via hot melt extrusion☆

Marzhan K. Akhmetova [a], Guzel K. Abilova [a,*], Aknaz B. Duisengali [a], Tomiris A. Nurlybaeva [a], Sanimai S. Uzakbaeva [a], Galiya S. Irmukhametova [b], Amirbek Z. Bekeshev [a], Vitaliy V. Khutoryanskiy [c,**]

[a] K. Zhubanov Aktobe Regional State University, 030000 Aktobe, Kazakhstan
[b] Al-Farabi Kazakh National University, Almaty 050040, Kazakhstan
[c] School of Pharmacy, University of Reading, Whiteknights, RG6 6AD Reading, United Kingdom

ARTICLE INFO

Keywords:
Poly(2-ethyl-2-oxazoline)
Polycarbophil
Hot melt extrusion
Mucoadhesion
Vaginal films
Metronidazole
Vaginal drug delivery

ABSTRACT

Mucoadhesive vaginal films are increasingly regarded as a versatile platform for local drug delivery, offering prolonged mucosal retention, ease of administration, and enhanced bioavailability. In this study, vaginal films based on blends of poly(2-ethyl-2-oxazoline) (POZ) and polycarbophil (PC) were developed and characterized, incorporating metronidazole as a poorly soluble antimicrobial drug. The films were prepared using hot-melt extrusion. Their physicochemical and mechanical properties, mucoadhesive performance, and ex vivo retention on the mucosal surface were studied. Particular attention was given to the effects of polymer ratio and plasticizer content on these characteristics. Key findings revealed that incorporating polycarbophil into POZ-based films significantly enhanced mucoadhesive strength, particularly in formulations containing glycerol as a plasticizer, which provided improved flexibility and adhesion. In *ex vivo* studies using sheep vaginal mucosa, POZ/PC films exhibited strong retention, with the POZ/PC (80:20) formulation showing significantly longer adhesion under simulated physiological fluid flow. Differential scanning calorimetry analysis confirmed partial amorphization of metronidazole in the films, reducing its crystallinity from 100 % to ~ 65–70 %. Additionally, the films provided sustained drug release and demonstrated notable antimicrobial activity against *S. aureus* and *E. coli*.

1. Introduction

Vaginal drug delivery represents an effective route of medication administration, providing both local and systemic therapeutic effects [1,2]. This method offers unique advantages: firstly, it allows drugs to bypass the first-pass hepatic metabolism; secondly, the relatively large surface area of the vaginal mucosa ensures rich blood flow [3]. However, the effectiveness of vaginal drug delivery may depend on factors such as the volume of vaginal secretions, pH levels, and the condition of the microbiota, which necessitates careful selection of the dosage form and formulation composition [4].

Mucoadhesive drug delivery systems have attracted significant attention due to their ability to enhance bioavailability and provide controlled drug release [5,6]. These systems use polymers that adhere to mucosal surfaces, extending the residence time and improving drug delivery [7]. They have been applied to various mucosal sites, including the oral cavity, gastrointestinal tract, eyes, nose, vagina, and rectum [8,9]. Mucoadhesion involves polymer wetting, chain interpenetration, and, in some cases, the formation of covalent bonds [10]. Various factors, including the properties of polymers, environmental conditions, volume of vaginal discharge, pH level and the status of the vaginal microbiota, affect the strength of mucoadhesion [11].

There are several types of dosage forms available for vaginal drug delivery, including creams, gels, suppositories, tablets, gelatin capsules and films [12–14]. Each form has its own advantages and limitations regarding ease of use, drug release rate, and dosing accuracy [15,16]. For example, creams and gels may be less convenient to use due to the risk of staining clothes and hands, as well as challenges with accurate

☆ This article is part of a special issue entitled: 'Poly(2-oxazoline)s' published in European Polymer Journal.

* Corresponding author at: K. Zhubanov Aktobe Regional State University, Aktobe 030000, Kazakhstan.
** Corresponding author at: Reading School of Pharmacy, University of Reading, Whiteknights, PO Box 224, RG6 6AD Reading, United Kingdom.
E-mail addresses: guzelab82@mail.ru (G.K. Abilova), v.khutoryanskiy@reading.ac.uk (V.V. Khutoryanskiy).

https://doi.org/10.1016/j.eurpolymj.2025.114175
Received 15 May 2025; Received in revised form 17 July 2025; Accepted 28 July 2025
Available online 29 July 2025

dosing, which can reduce the effectiveness of the therapy [17].

Vaginal films are a promising drug delivery system for contraceptive, antifungal, antimicrobial, or microbicide applications. They provide accurate dosing, rapid dissolution upon contact with vaginal fluids, and even distribution of the active ingredient [18,19]. Due to their flexibility and thin profile, these films are easy to insert and cause minimal discomfort for patients. Additionally, they ensure prolonged drug contact with the mucosal surface, which helps enhancing therapeutic effectiveness [20]. Recent developments in vaginal polymer films have shown promising advancements for drug delivery. Biopolymer films containing fluconazole and thymol have demonstrated improved anticandida activity, particularly against resistant *C. glabrata*, reducing the required fluconazole dose by 50 % [21]. Vaginal films containing tioconazole as an antifungal agent were developed to improve the treatment of vaginal candidiasis compared to the traditional egg-shaped formulation of this drug. Chitosan-hydroxypropyl methylcellulose films containing tioconazole demonstrated faster and more sustained antifungal activity against *Candida albicans* compared to the conventional tioconazole ovule formulation [22].

Vaginal films have proven effective for the local delivery of poorly water-soluble antimicrobial agents, such as metronidazole, and have been actively explored for the treatment of bacterial infections like bacterial vaginosis. For instance, hyaluronic acid-based films loaded with metronidazole were developed to improve bioadhesion and provide prolonged local drug release, showing enhanced therapeutic potential for vaginal delivery [23]. Another study focused on xanthan gum-based vaginal films, which also contained metronidazole and showed a promise for treating vaginal infections due to their mucoadhesive properties and sustained drug release [24]. These developments underscore the versatility of vaginal film platforms for effective localized drug delivery, including for poorly soluble antimicrobial agents. These systems combine the flexibility and mucoadhesion of gels with the stability and precision of solid forms, offering a versatile platform adaptable through various polymers and fabrication techniques.

Vaginal films are primarily produced using two methods: casting from solutions method and hot melt extrusion [25]. The casting method involves dissolving polymers and the active pharmaceutical ingredient in an appropriate solvent, followed by spreading the solution on a solid substrate and evaporating the solvent to form the film [26]. In contrast, hot melt extrusion involves mixing polymers and the active substance at an elevated temperature, followed by forming the film through an extruder [27,28]. Each of these methods has its own advantages and limitations, related to the physicochemical properties of the materials used and the characteristics of the final product.

To achieve the high quality and specific characteristics required in pharmaceutical polymer films, hot-melt extrusion (HME) has become an important method due to its efficiency, versatility, and control over film properties [29]. HME's appeal lies in its adaptability; it can produce films that meet diverse and demanding requirements, from drug stability to specific release profiles. The method is ideal for pharmaceutical applications, as it enables the development of films with defined physicochemical properties, which are essential for producing reliable and effective drug delivery systems [30]. By fine-tuning process parameters, HME supports the production of advanced polymer films that can be customized to achieve targeted release rates, enhanced bioadhesion, and optimized drug compatibility, making it an invaluable tool in pharmaceutical film manufacturing [31].

Poly(2-ethyl-2-oxazoline) has previously been demonstrated to be a suitable polymer for pharmaceutical formulations prepared via hot-melt extrusion, owing to its thermoplasticity [32–34], water solubility, biocompatibility, and ability to form films with good mechanical properties [35,36]. Some of the aforementioned studies also demonstrated the use of hot-melt extrusion to prepare poly(2-ethyl-2-oxazoline) blends with other polymers. However, due to its non-ionic nature, poly(2-ethyl-2-oxazoline) is generally expected to exhibit poor mucoadhesive properties. Therefore, blending it with a strongly mucoadhesive ionic polymer may be particularly advantageous for applications such as vaginal drug delivery.

In this study, hydrophilic polymer films were developed based on blends of poly(2-ethyl-2-oxazoline) (POZ) and polycarbophil (PC) using hot melt extrusion method. Polycarbophil, due to the presence of carboxyl groups, has excellent mucoadhesive properties, ensuring strong adhesion to mucosal surfaces [37–39]. The study examined films with different POZ to PC ratios (100:0, 90:10, and 80:20), as well as the inclusion of plasticizers – glycerol (GL) and polyethylene glycol (PEG) – to improve flexibility. The combination of these polymers allows to produce films with optimal properties for vaginal drug delivery. Evaluation of the physicochemical and mechanical properties, mucosal adhesion, and retention on *ex vivo* sheep mucosa showed that formulations with a POZ/PC ratio of 80:20 and the addition of glycerol exhibited the best flexibility and adhesion properties. To the best of our knowledge, the development of mucoadhesive vaginal films based on poly(2-ethyl-2-oxazoline) and polycarbophil blends via hot-melt extrusion represents a novel and promising strategy for creating effective vaginal drug delivery systems.

2. Experimental section

2.1. Materials

Poly(2-ethyl-2-oxazoline) (POZ, MW ~ 50 kDa, Sigma-Aldrich, Gillingham, UK) was used as the primary film-forming polymer due to its thermoplastic and hydrophilic nature. Polycarbophil (PC, Lubrizol Advanced Materials Europe, Belgium) served as a mucoadhesive agent. Glycerol (GL, ≥99.5 %, Sigma-Aldrich, UK) and polyethylene glycol 1500 (PEG 1500, Merck, Germany) were used as plasticizers. Sodium fluorescein (NaFl), metronidazole (MTZ, as a model poorly soluble antimicrobial drug), bovine serum albumin (BSA), glucose, urea, lactic acid, and acetic acid; all these chemicals were of analytical grade and obtained from Sigma-Aldrich (UK). A cellulose dialysis membrane tube (molecular weight cut-off 14 kDa) was obtained from Sigma-Aldrich (Gillingham, UK) was used for drug release experiments.

2.2. Preparation of the polymer films by HME technique

2.2.1. Preparation of polymer blend powders

Polymer solutions (4 % w/v) were prepared by dispersing blends of POZ and PC at weight ratios of 100:0, 90:10 and 80:20 in 500 mL of a water – ethanol mixture (60:40 v/v). The total polymer mass in each solution was 20 g. To enhance the elasticity and flexibility of the resulting films, two plasticizers – glycerol (GL) and polyethylene glycol 1500 (PEG 1500) – were added into the formulations. Optimal concentrations – 20 % (v/v) for glycerol and 30 % (v/v) for PEG 1500 – were selected based on preliminary experiments. Lower concentrations resulted in brittle or insufficiently elastic films, whereas higher concentrations led to excessive stickiness and impaired handling. Thus, the selected concentrations provided an optimal balance between flexibility, structural integrity, and ease of handling. The blends were stirred for up to 3 h to achieve complete homogenization, then poured into silicone moulds and dried in an oven at 50 °C for 24 h. The dried films were ground into a fine powder using a blender for 30 min to obtain blends suitable for extrusion. The aim of this step was to convert the dried polymer films into a particulate form suitable for feeding into the hot-melt extruder. The powders were visually assessed and found to be homogeneous, free from visible agglomerates, and adequately flowable. The resulting powder exhibited consistent behavior during extrusion, indicating sufficient uniformity for processing. The compositions of the polymer blends, including variations with and without plasticizers, are summarized in Table 1.

2.2.2. Hot-Melt extrusion of powdered blends

The prepared powdered blends were extruded using a hot-melt

Table 1
Composition of polymer blends for extrusion.

Sample	POZ (% w/w)	PC (% w/w)	PEG (% w/w)	GL (% w/w)
POZ (100)	100	–	–	–
POZ/PC (90:10)	90	10	–	–
POZ/PC (80:20)	80	20	–	–
POZ (100)/PEG	100	–	30	–
POZ/PC (90:10)/PEG	90	10	30	–
POZ/PC (80:20)/PEG	80	20	30	–
POZ (100)/GL	100	–	–	20
POZ/PC (90:10)/GL	90	10	–	20
POZ/PC (80:20)/GL	80	20	–	20

extrusion method. Each powdered blend (5 g) was loaded into the hopper of a twin-screw extruder equipped with co-rotating screws (Micro Compounder, DSM Xplore, Netherlands). The extruder was fitted with die 6 cm-wide and 0.2 mm-thick slit die to produce polymeric films. During the extrusion process, the polymer blends softened under the combined effects of heat (110–140 °C) and shear forces generated by the screw rotation, which was set to a speed of 75 rpm. The extrusion lasted for 5 min, during which the polymer samples became flexible and moved forward under pressure. The extruded films (size of approximately 5 cm in width and 10–12 cm in length) were cooled along a custom conveyor belt to a room temperature. The films were stored between silicone sheets to prevent sticking. In total, nine film samples were produced, including variations with and without plasticizers. These samples were then characterized and analyzed for their mechanical and mucoadhesive properties.

2.2.3. Preparation of sodium fluorescein (NaFl)-Loaded films

To prepare fluorescent films for *ex vivo* retention studies, sodium fluorescein (NaFl) was used as a model hydrophilic marker. A weighed amount of sodium fluorescein (1 % w/w relative to the total polymer mass) was dissolved in the polymer solution prior to the drying stage. The procedure followed was similar to that used for drug-free films: blends of POZ and POZ/PC (at 90:10 and 80:20 ratios) were plasticized with glycerol (20 % v/v), mixed thoroughly with NaFl, and poured into silicone molds. The samples were dried at 50 °C for 24 h. After drying, the films were milled into a fine powder and subjected to hot-melt extrusion, as described in Section 2.2.2. The resulting films were stored protected from light and moisture prior to analysis.

2.2.4. Preparation of Metronidazole-Loaded films

Drug-loaded polymer films based on POZ and POZ/PC, plasticized with glycerol, were prepared following the same general method as described for the drug-free formulations. The intended drug loading was approximately 36.7 % w/w. Metronidazole powder was added to the pre-optimized polymer solution and thoroughly mixed until fully homogenized. The resulting blends were cast into silicone molds.

While the film preparation process—such as polymer composition, casting technique, and extrusion—was initially optimized using drug-free formulations, additional adjustments were necessary upon incorporation of metronidazole to address drug-specific challenges. In particular, during the drying process, we observed that drying the drug-loaded films at the temperature optimized for blank formulations (50 °C) led to significant surface crystallization of metronidazole, with the formation of large visible crystals. To address this issue and enhance drug dispersion and content uniformity, the drying temperature was increased to 90 °C and maintained for 15 h. This adjustment resulted in smaller, more uniformly distributed drug crystals throughout the polymer matrix, as confirmed by visual inspection and microscopy analysis. It is important to emphasize that this change in drying temperature was required due to the specific crystallization behavior of metronidazole and did not affect the polymer composition or casting method.

After drying, the films were ground for 30 min using a blender to produce fine powder, followed by hot-melt extrusion as described previously. To minimize the risk of thermal degradation of metronidazole, slight reductions in extrusion temperature were applied compared to the drug-free blends. The optimized extrusion temperatures were as follows: 110 °C for POZ/PC (80:20), 100 °C for POZ/PC (90:10), and 90 °C for POZ (100). These adjustments were necessary to balance drug stability with the processability of the blends.

Thus, while the overall process was based on the optimized parameters from the blank formulations, further refinement was essential to accommodate the specific physicochemical properties of metronidazole. These modifications were validated through visual and microscopic analysis to ensure consistent film quality and drug distribution.

2.3. Characterization of the films

The studies presented in Section 2.3 were conducted on POZ- and POZ/PC-based films. Both plasticised and non-plasticized films were used in the analyses. Depending on the test method, circular samples of the required size were cut from the original rectangular films (5 × 5 cm^2). Drug-loaded films were additionally used for the DSC study in order to assess the crystallinity of the drug substance.

2.3.1. Thickness and weight uniformity

Film thickness and weight uniformity were evaluated using a digital micrometer and an analytical balance. Film thickness was measured at five different places on each sample, and the average thickness was then calculated. To evaluate the weight uniformity, five individual film samples (each with a diameter of 4.0 cm) were weighed separately, and the average weight was determined.

2.3.2. Folding endurance

Folding endurance was tested by selecting three random film samples. Each film was folded repeatedly at the same point until breakage occurred. The number of folds a film could withstand before breaking was recorded as its folding endurance.

2.3.3. Surface pH

Surface pH was determined by immersing a 10 mm diameter film sample in 5 mL of deionized water in a narrow, elongated beaker and allowing it to swell at room temperature for 30 min. The pH of the swollen film was then measured by gently inserting the pH meter electrode into the resulting solution using a FiveEasy Plus FP20 pH meter (Mettler-Toledo, Switzerland). The final pH value for each film was calculated as the mean ± standard deviation (n = 3).

2.3.4. Fourier transform infrared (FTIR) spectroscopy

The FTIR spectra of the dry films were recorded using a Cary 660 FTIR spectrometer (Agilent Technologies, USA) equipped with an attenuated total reflectance (ATR) accessory featuring a diamond crystal. The absorbance mode was employed, and the resolution was set at 1 cm^{-1}.

2.3.5. Thermogravimetric analysis (TGA)

The thermal stability of POZ, PC and POZ/PC films and dry powders was analyzed using TGA (NETZSCH TG 209F1 Libra, Germany). All samples (8–10 mg) were heated at 10 °C/min from 30 °C to 650 °C under a nitrogen atmosphere with a flow rate of 250 mL/min.

2.3.6. Differential scanning calorimetry (DSC)

Differential scanning calorimetry was used for both pure POZ and its blends POZ/PC to determine their glass transition temperature (T_g) and for metronidazole – loaded samples to assess the degree of crystallinity of the drug in the films. The measurements were carried out using a NETZSCH DSC 300 Caliris Select instrument (NETZSCH-Gerätebau GmbH, Selb, Germany) equipped with a cooling unit. Dry nitrogen at a flow rate of 60 mL/min was used as purge gas to ensure a controlled

atmosphere in the DSC cell.

The samples were analyzed in Tzero aluminum crucibles (NETZSCH-Gerätebau GmbH), with an empty crucible used as a reference. For T_g determination, samples of POZ and POZ/PC blends weighing up to 10 mg were initially cooled from room temperature to 0 °C, held at this temperature for 30 min, and then heated up to 180 °C at 10 °C/min. Subsequently, the samples were rapidly cooled back to 0 °C, held for another 30 min, and reheated to 180 °C. T_g was determined from the second heating curve using the reversing heat flow signals.

To assess the degree of crystallinity, polymer metronidazole – loaded film samples (9–10 mg) were placed in perforated Tzero aluminum pans and heated from 0 °C to 200 °C in a nitrogen atmosphere at a heating/cooling rate of 10 °C/min. The degree of crystallinity of metronidazole in each sample was determined from the specific enthalpy (ΔH) of the melting peak of the drug using Proteus® software (version 9.1.1, NETZSCH-Gerätebau GmbH) and calculated using the following equation [40,41]:

$$\textit{Degree of crystallinity}\ (\%) = \left(\Delta H_f \bullet \frac{w_f}{w_m}\right) \Big/ \Delta H_m \bullet 100 \quad (1)$$

where ΔH_f is the ΔH of the drug in the film, melting around 160 °C (melting point of the drug), ΔH_m is the ΔH of the pure crystalline drug, W_f is the film sample weight, and W_m is the weight of the drug in each sample.

2.3.7. Scanning electron microscopy (SEM)

SEM images of the film samples were acquired using a JSM-IT 200 instrument (JEOL Ltd., Japan). High-resolution imaging was achieved in a high-vacuum mode, using a secondary electron detector with an accelerating voltage of 20 kV. Prior to imaging, the sample surfaces were coated with a 20 nm thin layer of gold.

2.4. Mechanical analysis

The mechanical properties of the films, including puncture strength (PS), elongation at break (EB), and Young's modulus (E), were evaluated using a TA.XT Plus Texture Analyzer (Stable Micro Systems Ltd., UK) in a compression mode at room temperature. The testing methodology followed the procedure described in our previous study [42]. A schematic illustration of these measurements is presented in Fig. S1 (Supporting information). Briefly, film samples were secured in a specialized holder, and a spherical probe (P/5S) applied force until the material ruptured.

Equations (2)–(4) below were used to calculate the puncture strength (PS), percentage elongation at beak (EB) and Young's modulus (E) of each film, respectively [43,44]:

$$PS = \frac{Force}{Ar_s} \quad (2)$$

where Force is the maximum applied force recorded during strain.

$$EB = \left(\frac{\sqrt{a^{\cdot 2} + b^2} + r}{a} - 1\right) \times 100\% \quad (3)$$

where a ′ is the initial length of the film sample; b is the penetration depth/vertical displacement by the probe; r is the radius of the probe; and a is the radius of the film in the sample holder opening.

$$E = \frac{\Delta\sigma}{\Delta\varepsilon} \quad (4)$$

where Δσ is change in the stress; Δε is the change in strain.

All tests were performed in triplicates, and the results were reported as mean values ± standard deviations, followed by statistical evaluation.

2.5. Evaluation of mucoadhesive properties

2.5.1. Preparation of simulated vaginal fluid

Simulated Vaginal Fluid (SVF) was prepared to replicate physiological conditions for experiments on the mucoadhesive properties of the films, following the formulation described in our previous study [45]. Briefly, the solution was prepared by dissolving the necessary components in distilled water, ensuring complete dissolution, and adjusting the pH to 4.2 to closely mimic the natural vaginal environment. The SVF was stored at 4 °C and used within 24 h. Throughout the mucoadhesion experiments, the SVF solution was kept at 37 °C using a water bath to ensure consistent physiological conditions.

2.5.2. Ex vivo mucoadhesion studies on sheep vaginal mucosa

The mucoadhesive properties of the films were assessed using a tensile method on sheep vaginal mucosa, following the approach described in our previous studies [42,45]. The experiments were conducted with a Texture Analyzer XT Plus (Stable Micro Systems Ltd., UK) equipped with a 10 mm cylindrical aluminum probe (P/10). Circular film discs (10 mm in diameter) were attached to the probe using a double-sided adhesive tape, which was securely fixed to the movable arm of the instrument.

Fresh sheep vaginal tissues were obtained from a local slaughterhouse (Altyn-Orda, Almaty, Kazakhstan) shortly after animal slaughter and transported to the laboratory in cold containers. The tissues were carefully dissected into 5 × 5 cm sections using sterile blades, ensuring that the inner mucosal surface remained uncontaminated. To preserve their structural integrity, the tissues were stored at 4 °C and used within 24 h.

The experimental setup included a platform with a central hole (15 mm in diameter) and clamps to secure the mucosal tissue in place. Before testing, the mucosal surface was moistened with SVF to simulate physiological conditions and prevent dehydration. The film samples were then brought in contact with the tissue for 30 s, after which the probe was retracted until complete detachment occurred. A schematic illustration of these measurements is presented in Fig. S2 (Supporting information).

The test parameters were as follows: pre-test speed of 0.5 mm/s, test speed of 0.5 mm/s, post-test speed of 10.0 mm/s, applied force of 100 g, return distance of 10 mm, contact time of 30 s, automatic trigger mode, and a trigger force of 0.049 N. Each experiment was repeated five times using different tissue samples to ensure reproducibility.

Key parameters, including the maximum detachment force (F_{adh}) and the total work of adhesion (W_{adh}), calculated as the area under the force/distance curve, were analyzed to assess the films' mucoadhesive behavior.

2.5.3. Ex vivo retention studies on sheep vaginal mucosa

The retention of mucoadhesive films on vaginal surface was evaluated using a fluorescence microscopy flow through method as described in [46]. For retention assessment, fluorescent POZ and POZ/PC films plasticized with glycerol were used, based on previous studies investigating their mechanical and mucoadhesive properties using a texture analyzer. These studies demonstrated that glycerol incorporation enhances the films' mechanical strength and adhesion to the mucosal surface.

A digital USB microscope with up to 1000 × magnification (StreamCam Full HD, Logitech, China) was used for image acquisition and a UV LED flashlight (395 nm wavelength) was used as an external UV light source. The UV flashlight was only activated during image capture to prevent continuous sample and tissue exposure to UV light.

Fresh sheep vaginal tissues were obtained from a local slaughterhouse (Aktobe, Kazakhstan) immediately after animal slaughter, transported to the laboratory in chilled containers, and used within 24 h. The tissues were carefully prepared with sterile disposable blades, ensuring no contact with the inner mucosal layer, and cut into rectangular

sections (~2 × 7 cm). Until use, the vaginal tissue samples were stored at 4 °C in Petri dishes wrapped in a cling-film to prevent dehydration.

Each experiment was conducted at 37 °C and under high humidity to simulate physiological conditions. Before the experiment, tissue samples were fixed onto microscopy glass slides at a 45° angle and moistened with SVF. Spherical polymer discs (4 mm in diameter) loaded with sodium fluorescein (NaFl) were then placed on the moistened tissue and irrigated with SVF (pH 4.2) at a flow rate of 100 μL/min for 100 min, controlled by a syringe pump. At the beginning of a retention experiment, baseline images of clean vaginal tissue were captured to determine the initial fluorescence intensity for each sample. Fluorescent images were then taken at specific time intervals and analyzed using ImageJ software.

The fluorescence intensity was calculated using the following equation [47]:

$$Fluorescence\ intensity = \frac{I - I_b}{I_0 - I_b} \quad (5)$$

where I_b is the background fluorescence intensity of the blank tissue; I_0 is the initial fluorescence intensity (at the zero time point, before the first washing, considered as 100 % fluorescence); and I is the fluorescence intensity after each wash. These fluorescence values were then converted into percentage mucosal retention values, allowing the evaluation of the film's ability to retain on the mucosal surface over time.

2.6. Characterization of the drug-containing films

2.6.1. Determination of metronidazole content in polymer films

To determine the amount of metronidazole in POZ and POZ/PC films, 4 mm diameter samples with an average weight of 3.6 mg were placed in 100 mL of distilled water and allowed to fully dissolve. Once the films had completely dissolved, the solution was filtered, and 1 mL aliquot was collected for analysis. The absorbance was measured using UV–Vis spectroscopy (UV-1900, Shimadzu, Japan) at 320 nm. A standard calibration curve was used to determine the metronidazole concentration (Fig. S3, Supporting information). Each measurement was performed three times, and the percentage of the drug content in the films was calculated accordingly.

2.6.2. Polarized light microscopy

The structure of drug-loaded polymer films was analyzed using a polarized light microscope CX40P-RT (Ningbo Sunny Instruments Co., Ltd., China) in a reflection mode to detect and characterize crystalline metronidazole. Images were captured using a digital camera with 50 × magnification.

2.6.3. In vitro metronidazole release

The drug release from the films was evaluated using a Franz diffusion cell under sink conditions, following our previously described protocol [45]. A cellulose membrane served as a barrier between the donor and acceptor compartments, with SVF used as the release medium. The receptor chamber contained 34 mL of SVF, stirred at 80 rpm and maintained at 37 °C throughout the experiment.

The films were placed directly on the dialysis membrane in the donor compartment without prior wetting. At predetermined time intervals, 1 mL aliquots were withdrawn from the receptor chamber and replaced with a fresh SVF to maintain a constant volume. The experiment lasted 5 h, with each film type tested 5 times.

The amount of the drug released at each time interval was quantified using a UV–Vis spectrophotometer UV-1900 (Shimadzu, Japan) at 320 nm. Data analysis was performed using LabSolutions UV–Vis software based on a pre-established calibration curve ($R^2 = 0.99953$). A standard calibration curve generated in SVF was used to determine the metronidazole concentration (Fig. S4, Supporting information). Each experiment was performed in triplicate, and the mean ± standard deviation values were calculated.

2.6.4. Antimicrobial studies

The antibacterial activity of POZ/GL (100), POZ/PC/GL (90:10), and POZ/PC/GL (80:20) films, with and without metronidazole, was evaluated in the Microbiology Laboratory of JSC "Scientific Center for Anti-Infective Drugs" (Almaty, Kazakhstan). The tests were performed against *Escherichia coli* ATCC 8739 (Gram-negative) and *Staphylococcus aureus* ATCC 6538-p (Gram-positive) bacteria using the standard agar disc-diffusion method [45,48].

Briefly, bacterial cultures were first seeded on nutrient agar, and the inhibition zones around the film samples were measured to assess their antimicrobial effect. Active bacterial colonies were suspended in 5 mL of saline solution (0.9 % NaCl) and adjusted to a turbidity of 0.5 McFarland standard (1.5×10^8 CFU/mL). The bacterial suspension (1.5–2.0 mL) was then evenly spread across nutrient agar plates using a sterile cotton swab.

For the disc-diffusion assay, circular film samples (6 mm in diameter, drug content ~ 22.0 ± 0.3 mg for metronidazole-loaded films) were placed onto the agar surface using sterile forceps. A sterile paper disc (HiMedia Laboratories, India) loaded with pure metronidazole (22 mg) served as a positive control.

For the well-diffusion assay, wells of 6 mm diameter were punched into the agar and each filled with 50 μL of metronidazole solution (22 mg per well). Plates were incubated at 37 °C for 24 h. After incubation, the diameter of the inhibition zones (including disc/well diameter) was measured to evaluate bacterial susceptibility.

2.7. Statistical analysis

The results are presented as mean values ± standard deviation. Data were analyzed for statistical significance using a two-tailed Student's *t*-test, with a p-value of less than 0.05 considered statistically significant. All statistical analyses were performed using Microsoft Excel with the Analysis ToolPak add-in. One-way analysis of variance (ANOVA) was used to assess differences between groups in the drug release experiments, followed by post-hoc analysis using Welch's *t*-test.

3. Result and discussion

3.1. Preparation and Characterisation of POZ and POZ/PC blend films

The films based on POZ and its blends with PC were successfully prepared using hot-melt extrusion technique. The physical appearance of the films varied slightly depending on the presence of plasticisers. Films without plasticisers were noticeably more rigid and brittle, whereas the incorporation of PEG or GL markedly improved the flexibility and elasticity of the samples, resulting in greater pliability and durability. The physicochemical parameters, including film thickness, weight, surface pH, and folding endurance, are summarised in Table 2.

The film thicknesses varied depending on the composition and the presence of plasticisers, with the values in the range of 0.183 ± 0.012 to 0.278 ± 0.010 mm. The addition of PEG did not affect the thickness of the films significantly ($p < 0.05$); however, an inclusion of GL increased the sample thickness by approximately 22–31 %, which may be due to some swelling induced by this plasticiser.

Flexibility is a crucial factor for films intended for vaginal administration, as the material must be able to conform to the application site without a risk of breaking and harming a sensitive tissue. One way to assess this flexibility is through folding endurance testing, which measures the number of folds a film can withstand without tearing. According to the existing literature [49,50], films with a folding endurance value greater than 300 folds are considered to have excellent flexibility. In our study, the POZ and POZ/PC films with plasticisers showed great flexibility, withstanding more than 300 folds without breakage. The films without plasticisers, however, demonstrated a lower folding

Table 2
Physicochemical parameters of POZ and POZ/PC blend films.

Sample	Thickness (mm)	Weight (mg)*	pH	Folding Endurance
POZ (100)	0.190 ± 0.010	0.006 ± 0.002	6.47 ± 0.02	<300
POZ/PC (90:10)	0.213 ± 0.015	0.007 ± 0.001	5.28 ± 0.06	<300
POZ/PC (80:20)	0.183 ± 0.012	0.007 ± 0.002	5.04 ± 0.13	<300
POZ (100)/PEG	0.203 ± 0.021	0.008 ± 0.001	6.75 ± 0.60	>300
POZ/PC (90:10)/PEG	0.193 ± 0.015	0.008 ± 0.002	5.02 ± 0.12	>300
POZ/PC (80:20)/PEG	0.190 ± 0.010	0.008 ± 0.001	4.98 ± 0.05	>300
POZ (100)/GL	0.232 ± 0.009	0.008 ± 0.001	6.62 ± 0.03	>300
POZ/PC (90:10)/GL	0.278 ± 0.010	0.009 ± 0.002	6.34 ± 0.13	>300
POZ/PC (80:20)/GL	0.233 ± 0.003	0.008 ± 0.002	6.03 ± 0.02	>300

Note: All values are presented as mean ± SD (n = 3).
* Circular samples of 10 mm were weighed.

endurance, suggesting reduced flexibility compared to their plasticised counterparts.

The pH values of the film surfaces ranged from 4.98 ± 0.05 to 6.75 ± 0.60, with a slightly acidic to neutral profile consistent with the polycarbophil content in the blends. This mild acidity aligns well with the vaginal pH environment, which is also weakly acidic, suggesting that these films are suitable for intravaginal application and are unlikely to disrupt the natural vaginal pH.

The films displayed a smooth and uniform appearance, with plasticized variants demonstrating slightly enhanced flexibility. These observations support the conclusion that POZ and POZ/PC films, particularly those containing plasticizers, possess both the desired mechanical flexibility and surface pH compatibility for potential vaginal applications.

3.2. Fourier transform infrared spectroscopy

Fourier transform infrared spectroscopy (FTIR) is powerful technique for studying intermolecular interactions and structural changes in polymer blends. Previous studies on the interaction of poly(2-ethyl-2-oxazoline) with chitosan in their blends have shown that the carbonyl groups (C=O) of POZ act as proton acceptors in relation to the hydroxyl groups of chitosan and form hydrogen bonds [51].

Polycarbophil, a lightly crosslinked polyacrylic acid, contains carboxyl groups that can act as proton donors to the carbonyl groups of POZ, facilitating intermolecular hydrogen bonding. To investigate the nature of interactions between these two polymers, FTIR spectra of poly (2-ethyl-2-oxazoline) and its blends with polycarbophil were recorded (Fig. 1). Due to technical difficulties associated with the extrusion process, it was not possible to prepare a film from pure polycarbophil, necessitating the analysis of this polymer in a powder form. The FTIR spectra of pure POZ were recorded both in powder and film forms.

The FTIR spectra of pure POZ revealed characteristic peaks corresponding to its functional groups. The main band of the carbonyl group (C=O) of the amide bond was observed at 1635 cm^{-1} in the spectra of dry POZ, which is consistent with literature data [52]. In the POZ film, this peak shifted to 1631 cm^{-1}, likely due to the different residual moisture content in these samples. Indeed, a broad absorption peak at 3392 cm^{-1} appeared in the spectrum, indicating the presence of bound water that was not fully removed during the film preparation.

The FTIR spectrum of polycarbophil exhibits a characteristic peak of the carbonyl group (C=O) at 1702 cm^{-1}, corresponding to the stretching of carbonyl bonds in the carboxyl groups of polyacrylic acid. A broad band in the range of 2800–3600 cm^{-1}, centered around 2925 cm^{-1}, suggests strong hydrogen bonding and O–H stretching in the carboxyl groups, which is typical for this polymer.

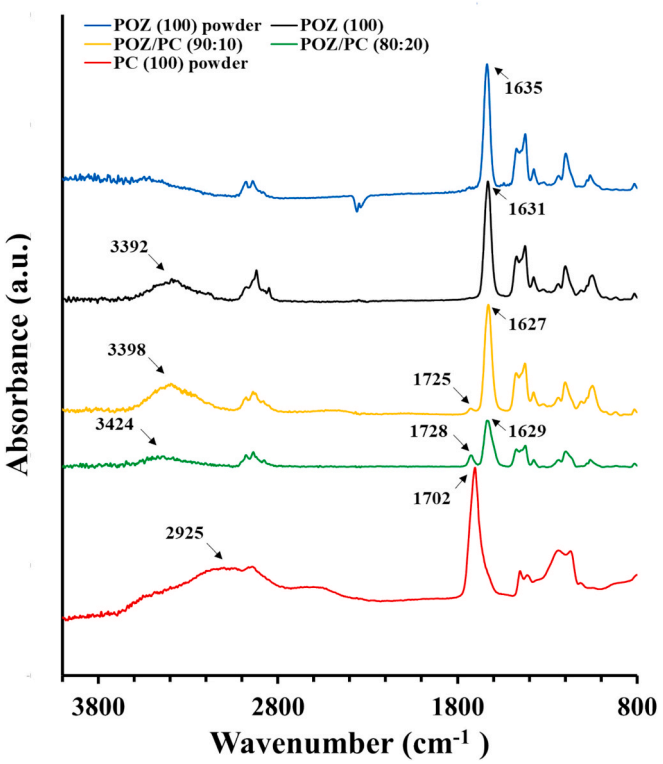

Fig. 1. FTIR spectra of pure POZ, PC and their blends. Spectra were vertically offset for visual clarity. Original absorbance values are presented without normalization.

The FTIR spectra of POZ/PC blends show the characteristic bands of both components, but the intensity and shape of the peaks depend on the polymer ratio in the blend. In the blends, the absorption band of the carbonyl group of POZ shifts to lower wavenumbers: 1627 cm^{-1} for the POZ/PC (90:10) blend and 1629 cm^{-1} for the POZ/PC (80:20) blend. These shifts suggest the likely formation of intermacromolecular hydrogen bonds between the amide carbonyl groups of POZ and the carboxyl groups of polycarbophil (−C=O···HOOC–). Moreover, the spectra of the blends show notable changes in the O–H stretching region and the carbonyl (C=O) band of the carboxyl group in polycarbophil, indicating a redistribution of hydrogen bonds upon polymer blending.

In conclusion, the results of FTIR spectroscopy indicate that intermolecular interactions occur between poly(2-ethyl-2-oxazoline) and polycarbophil, primarily through hydrogen bonds between the carbonyl and carboxyl groups.

3.3. Thermogravimetric analysis (TGA)

Thermogravimetric analysis was used to evaluate the thermal stability and degradation behavior of the polymer blends in response to increasing temperature. The results of TGA analysis of the samples prepared in this study are shown in Fig. 2. The TGA curve of the POZ film shows an initial weight loss in the 80–135 °C range, which corresponds to the evaporation of residual moisture. This is followed by a major degradation step at approximately 404 °C. The presence of the initial weight loss suggests incomplete drying during film preparation, which is common for hydrophilic polymers. Unlike the dry POZ powder, which shows a single-step degradation at 425 °C, the film exhibits a two-phase profile due to this initial water loss. However, POZ, as in the previous reports [42,53], also demonstrates high thermal stability. It is

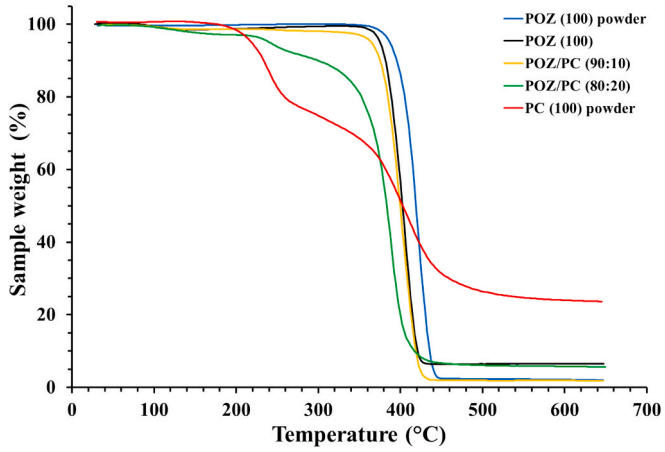

Fig. 2. TGA thermograms of pure POZ, pure PC and POZ/PC blend films.

interesting to note that POZ prepared in the form of a film exhibits a higher level of undegradable residue compared to the original POZ powder. The exact reasons for this difference are not fully clear, but it may be associated with the formation of denser macromolecular packing or thermally stable structures during the film extrusion process, possibly promoted by the presence of moisture in the initial sample.

For PC in dry powder form, degradation occurs in two distinct steps, with the highest degradation rates observed at 230 °C and 385 °C. This two-step degradation is related to initial decarboxylation and subsequent breakage of C–C bonds, as previously reported [54,55]. The residual mass of approximately 36 % observed at 600 °C likely represents carbonaceous char residue, commonly formed during thermal decomposition of polyacrylic acid-based materials [56].

In the case of POZ/PC blends, a moisture loss is observed in the temperature range of 80 – 150 °C similarly to the pure POZ films. Furthermore, a downward shift in temperature in the second degradation stage is observed, with the highest degradation rate observed at 402 °C for the 90:10 blend and 389 °C for the 80:20 blend. These results indicate that the incorporation of PC into POZ films reduces their heat resistance, consistent with lower temperature stability of pure PC. A three-stage weight-loss profile is observed in the 80:20 blend, which shows the features typical for both polymers. The levels of undegradable residue in the blends are consistent with their PC content; the sample containing 20 % PC shows a higher residue compared to the sample with 10 % PC.

3.4. Differential scanning calorimetry (DSC)

DSC analysis was performed to evaluate the compatibility of POZ and PC in their blends. The appearance of a single glass transition temperature (T_g), situated between the T_g values of the individual components, generally suggests complete miscibility between the polymers in a blend. The DSC thermograms in Fig. 3a show the presence of single T_g, which vary depending on the polymer blend composition.

The T_g of PC (in a powder form) was recorded at 136 °C, typical for crosslinked polyacrylic acids [54]. The T_g values for POZ in powder and film form were determined at 56 °C and 55 °C, respectively, which aligns well with previously published data [51]. Incorporating PC into the blend and increasing its proportion led to marked T_g changes, with T_g values rising alongside the PC content. Specifically, POZ/PC (90:10) and POZ/PC (80:20) exhibited T_g of 61 °C and 87 °C, respectively.

Fig. 3b shows the dependence of the glass transition temperature (T_g) on the mass fraction of POZ, obtained experimentally and calculated theoretically using the following equations [57]:

$$\text{Fox Equation}: \quad \frac{1}{T_g} = \frac{W_{POZ}}{T_{g_{POZ}}} + \frac{W_{PC}}{T_{g_{PC}}} \tag{6}$$

$$\text{Gordon} - \text{Taylor Equation}: \quad T_g = \frac{W_{POZ}T_{g_{POZ}} + kW_{PC}T_{g_{PC}}}{W_{POZ} + kW_{PC}} \tag{7}$$

where W_{POZ} and W_{PC} are the weight fractions of POZ and PC, respectively; and $T_{g_{POZ}}$ and $T_{g_{PC}}$ are the glass transition temperatures of POZ and PC, respectively; k is the ratio of heat capacity change of PC over POZ [$k = \Delta(\frac{C_{p2}}{C_{p1}})$].

As can be seen, increasing the POZ content leads to a decrease in the glass transition temperature, consistent with the typical behavior for polymer blends with differing T_g values.

The theoretical values calculated using the Fox and Gordon-Taylor equations closely follow the general trend; however, the experimental data show partial upward deviation from the predicted curves. This deviation may suggest the presence of specific interactions between the blend components – such as hydrogen bonds – which enhance compatibility beyond what would be expected from a simple physical blend.

These results are consistent with previous studies on similar polymer systems, such as POZ and Carbopol® 971 interpolymer complexes reported by Moustafine et al [52]. This study found that Carbopol® 971, similarly to PC, forms strong hydrogen bonds with POZ in interpolymer complexes, resulting in a single, composition-dependent T_g. However, in physical blends (without complexation), two distinct T_g values were observed, indicating phase separation and reduced miscibility [52].

In the present study, the DSC analysis demonstrates that the detection of a single T_g in extruded POZ/PC films indicates significant

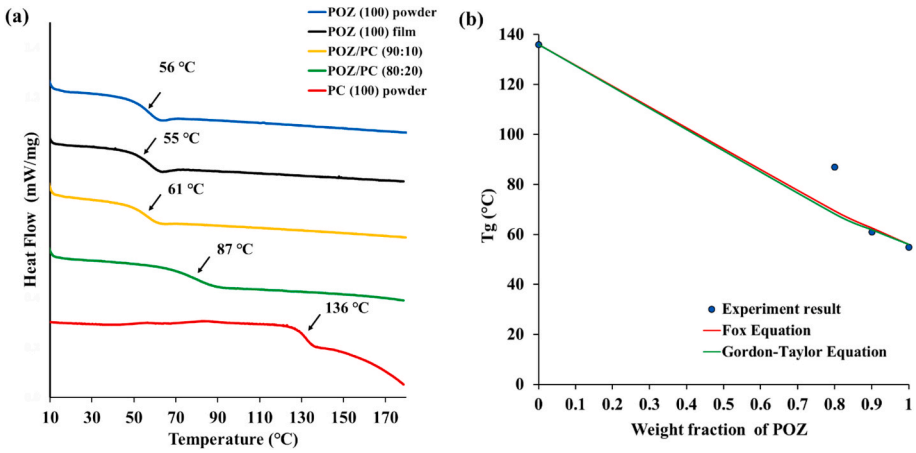

Fig. 3. DSC thermograms of pure POZ, pure PC and POZ/PC blend films in various ratios (a) and T_g of experimental results compared with theoretical data (b).

molecular-level interactions and miscibility between the polymers, likely due to hydrogen bonding between the carboxyl groups of PC and the carbonyl and amide groups of POZ. These interactions restrict polymer chain mobility to some extent and enhance the stability of the resulting films.

3.5. Scanning electron microscopy

Scanning electron microscopy (SEM) was used to examine the surface and cross-sectional morphology of POZ and POZ/PC films. Fig. 4 presents SEM images of the film surfaces (A) and cross-sections (B and C) at different magnifications. The SEM images of POZ (100), POZ/PC (90:10), and POZ/PC (80:20) films reveal relatively smooth and homogeneous surface morphology, with no visible signs of phase separation. The cross-sectional images display a well-integrated structure with minimal textural variations, indicating a good degree of phase compatibility between POZ and PC. As the PC content in the blend increases, the surface appears even smoother, which aligns with the DSC data showing an increased T_g, suggesting stronger interactions between POZ and PC components.

The surface morphology of POZ/PC (80:20) films plasticized with GL and PEG appears smooth and homogeneous, with no signs of phase separation in the glycerol-plasticized films. Cross-sectional analysis of the POZ/PC (80:20)/GL films reveals a cohesive and flexible structure, consistent with the role of glycerol in enhancing chain mobility and flexibility within the polymer matrix. By contrast, although PEG-plasticised POZ/PC (80:20) films retain an overall smooth surface, they display distinct cracks that are absent from the other formulations. The cross-section of the PEG-plasticized film displays a layered structure with minor indications of phase separation, likely due to uneven distribution of PEG within the polymer matrix, resulting in a slightly less cohesive blend compared to glycerol. This partial phase separation may influence the mechanical properties of the film, potentially making it less flexible than the glycerol-plasticized films. The presence of surface cracks suggests that PEG might lead to localized stress points within the matrix, which could affect the durability and flexibility of the films under mechanical stress. These variations in structural integrity might impact the suitability of these films for applications requiring prolonged stability and flexibility in a moist environment.

3.6. Mechanical analysis

The mechanical properties of POZ/PC films were analyzed to determine their suitability for biomedical applications, where both strength and flexibility are key factors. Results for puncture strength, elongation at break, and Young's modulus are displayed in Fig. 5.

For puncture strength (Fig. 5a), pure POZ films performed the best, while adding PC gradually reduced this strength, particularly in the POZ/PC (90:10) and POZ/PC (80:20) blends. This decline is likely due to PC's rigid and brittle nature, which can lead to structural inhomogeneity and make the films more prone to microcracks under pressure. Glycerol-plasticized films showed a marked increase in puncture strength, likely due to improved chain mobility and an overall more flexible structure. On the other hand, films with PEG displayed a slight drop in the puncture strength, potentially due to phase separation and uneven PEG distribution, as observed in SEM images [58,59].

The trend in the elongation at break (Fig. 5b), which reflects the films' flexibility, followed a similar pattern. Pure POZ had moderate elongation, which decreased as more PC was added, suggesting a drop in elasticity. Glycerol-plasticized films, particularly POZ/PC (80:20)/GL, showed the highest elongation, underscoring glycerol's strong role in boosting macromolecules flexibility. PEG also improved elongation but to a lesser extent than glycerol, likely due to structural imperfections seen in SEM and PEG's uneven distribution within the polymer blend [59].

The Young's modulus measurements (Fig. 5c) showed that pure POZ films had a low modulus, highlighting their inherent flexibility. An increase in PC content corresponded with a rise in modulus, consistent with the higher glass transition temperatures (T_g) observed in the DSC thermograms. This suggests that stronger intermolecular interactions and restricted chain movement occur with higher PC content [39,60]. Glycerol significantly lowered the modulus, making the films softer and more pliable, an advantage for materials used in deformative environments. PEG-plasticized films, however, exhibited only a slight reduction in the modulus values, likely because of partial phase separation and decreased cohesion within the matrix [58].

Overall, these findings show that both the composition and choice of plasticizer significantly influence the mechanical properties of POZ/PC films. Glycerol stands out for its effectiveness in enhancing both flexibility and puncture strength, making it an ideal plasticizer for applications requiring durability and elasticity. PEG also contributes to elasticity but may compromise uniformity in mechanical properties, an

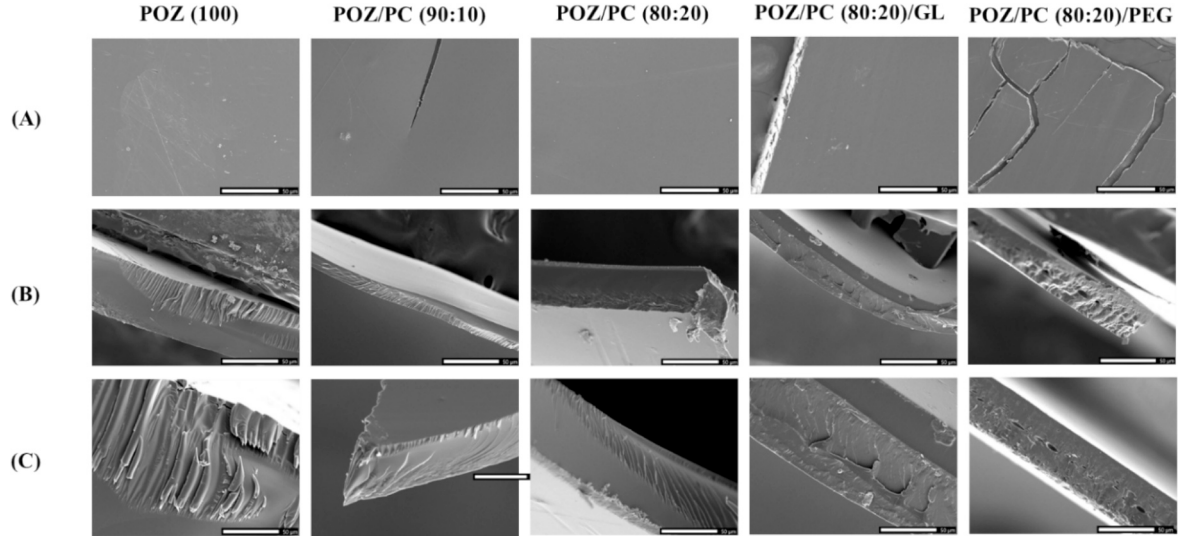

Fig. 4. SEM images of pure POZ film and POZ/PC blend films (A) surface and (B,C) cross- sections at different magnifications: (A,B) magnification × 300; (C) magnification × 500. Scale bars are 50 μm.

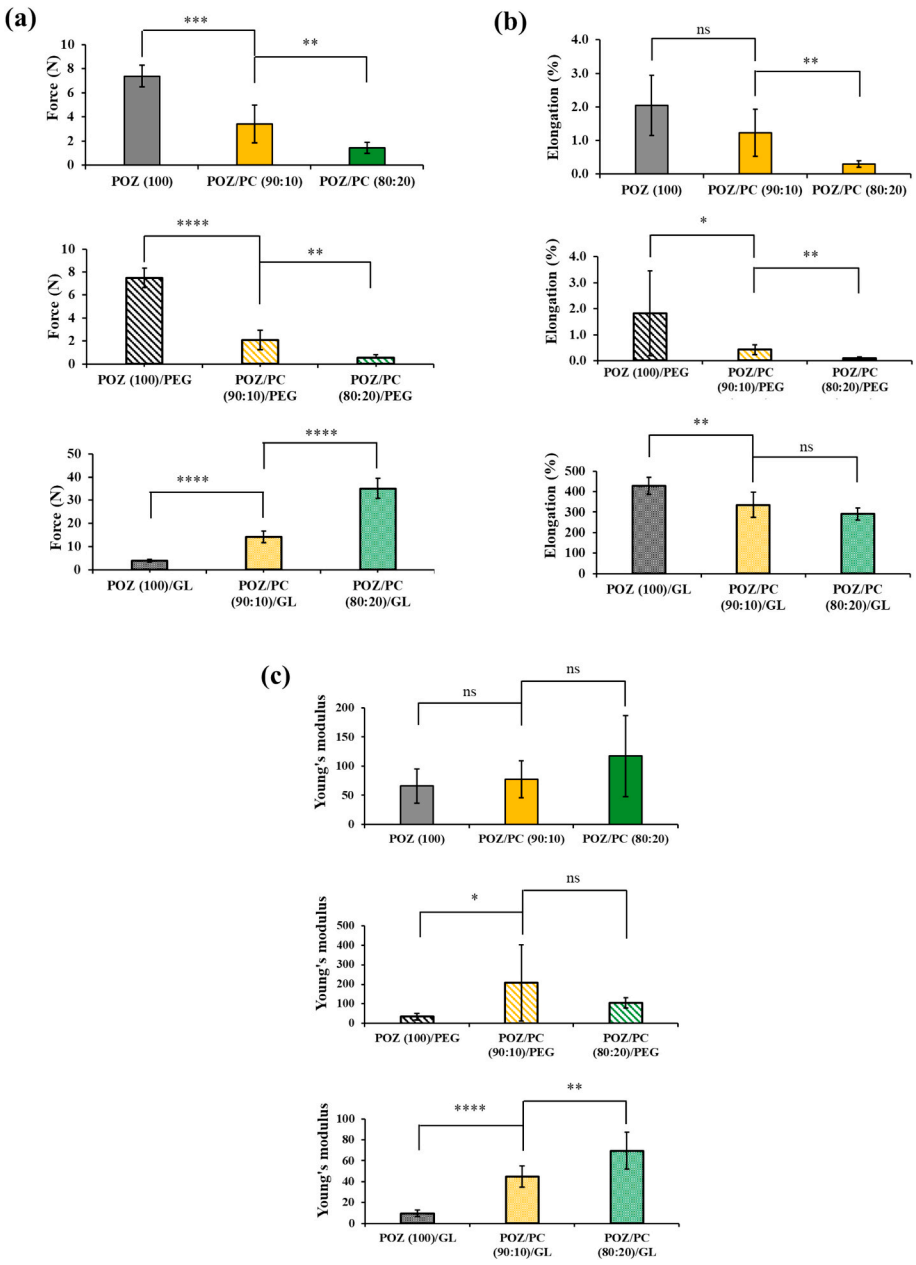

Fig. 5. Mechanical analysis of pure POZ film and POZ/PC blend films with and without plasticizer: Force (a), elongation at break (b) and Young's modulus (c). Data are expressed as mean ± standard deviation (n = 5). Statistically significant differences are given as: * – $p < 0.05$; ** – $p < 0.01$; ***—$p < 0.001$; ****—$p < 0.0001$; ns—no significance.

important consideration when selecting plasticizers.

3.7. Ex vivo mucoadhesion studies on sheep vaginal mucosa

Mucoadhesive properties of POZ and POZ/PC films play a key role in ensuring effective retention on mucosal surfaces, which is critical for vaginal drug delivery. Examination of detachment force and work of adhesion provides better understanding of the strength of interactions between the films and mucosal surface. Fig. 6 shows these values, illustrating how both polymer composition and plasticizer type shape the mucoadhesive characteristics of the films.

Pure POZ films initially showed modest mucoadhesion, with a detachment force of 0.88 ± 0.20 N. However, addition of glycerol significantly boosted mucoadhesive strength across all film compositions. For instance, POZ (100)/GL displayed nearly a four-fold increase in mucoadhesive strength (4.57 ± 0.38 N) compared to non-plasticized POZ (100). This increase is likely attributed to glycerol's ability to enhance polymer chain flexibility, allowing closer contact with the mucosal surface, more efficient diffusion of macromolecules of the polymer into the mucus, formation of an interpenetration layer and stronger interactions between the carbonyl groups in the POZ and the vaginal mucosal surface. In contrast, using polyethylene glycol (PEG) as a plasticizer produced a moderate effect, as shown by POZ (100)/PEG (1.31 ± 0.32 N), and even seemed to reduce mucoadhesive properties in POZ/PC blends. This reduction may be due to PEG's larger molecular size, which could limit its ability to form strong hydrogen bonds with the mucosal surface.

Although polycarbophil generally provides stronger mucoadhesion due to its anionic nature [39], adding PC to POZ films did not substantially enhance the mucoadhesive properties as expected. For non-plasticized POZ/PC films, detachment force measurements showed that increasing the PC content did not improve mucoadhesion, and for

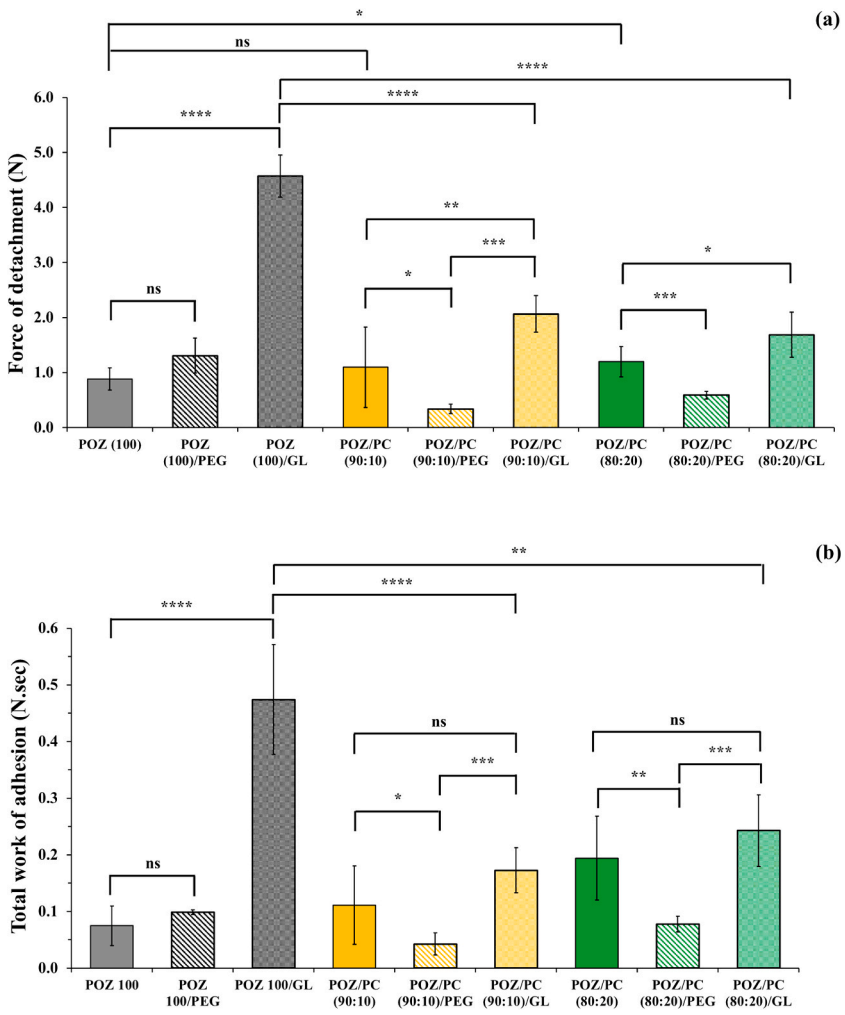

Fig. 6. Force of detachment F_{adh} (a) and total work of adhesion W_{adh} (b) values for the detachment of plasticized and non-plasticized POZ and POZ/PC blend films from the sheep vaginal mucosa. Data are expressed as mean ± standard deviation (n = 5). Statistically significant differences are shown as: * – $p < 0.05$; ** – $p < 0.01$; ***—$p < 0.001$; ****—$p < 0.0001$; ns—no significance.

plasticized films, it even slightly reduced these properties. This outcome may be related to the relatively low amount of polycarbophil used in these blends, which might not be enough to form a firm adhesive interface with the mucosal tissue.

The work of adhesion results mirror the trends with the values of the force of detachment, with POZ (100)/GL reaching the highest value (0.47 ± 0.09 N·sec), indicating strong and lasting interactions with the mucosal surface. PEG-plasticized films, on the other hand, showed lower work of adhesion in all formulations, highlighting glycerol's effectiveness in enhancing mucoadhesive properties.

3.8. *Ex vivo retention studies on sheep vaginal mucosae*

The ability of polymer films to adhere to and retain on mucosal surfaces over an extended period is crucial for effective vaginal drug delivery, particularly for applications that require localized treatment. Retention studies allow us to gauge how well these films stick to mucosal surfaces under conditions that mimic the human body. In this study, we looked at how well glycerol-plasticised films of POZ and POZ/PC, loaded with sodium fluorescein (NaFl) as a fluorescent marker, adhered to ex vivo sheep vaginal tissue. This method, adapted from previously validated ex vivo retention tests [44], uses fluorescent imaging to track how the films hold up under continuous fluid flow.

The fluorescent images in Fig. 7a give a clear picture of how retention of the films on vaginal mucosa changes over time. These images highlight that POZ/PC blends hold up better than pure POZ films. Over time, the POZ/PC (80:20) films retain more of their fluorescent signal, even at the 60 and 100-minute intervals, while the pure POZ (100) films quickly lose their retention. This difference might be due to the hydrophilic nature of POZ, which can cause the film to swell and loosen in the presence of water, leading to a quicker dissolution and wash-off. Additionally, while glycerol initially improves mucoadhesion by increasing polymer chain mobility, it also allows water to penetrate into a film more rapidly, which might explain why it does not hold up as well during the longer exposure to simulated vaginal fluid.

Fig. 7b shows the retention patterns of POZ (100)/GL, POZ/PC (90:10)/GL, and POZ/PC (80:20)/GL on sheep vaginal mucosa, under a steady flow of simulated vaginal fluid. Right at the start (0 min), all films were set to 100 % retention, corresponding to their initial fluorescence on the mucosal surface. In the first few minutes, a slight increase in fluorescence above 100 % can be noticed, likely due to the films' hydration, which boosts the dye fluorescence. This observation matches with the previous reports [51], which also recorded increased fluorescence upon initial hydration. By 10 min, the films begin showing noticeable differences in fluoresceine retention. For example, the POZ (100)/GL film retention dropped to 47 ± 12 %, whereas POZ/PC (80:20)/GL remained longer, with around 125 ± 11 % ($p < 0.001$). At the 60-minute mark, POZ (100)/GL retention was down to 10 ± 5 %, while POZ/PC (80:20)/GL held at 44 ± 8 % ($p < 0.05$). At the end of 100 min, the POZ (100)/GL film had almost completely washed away,

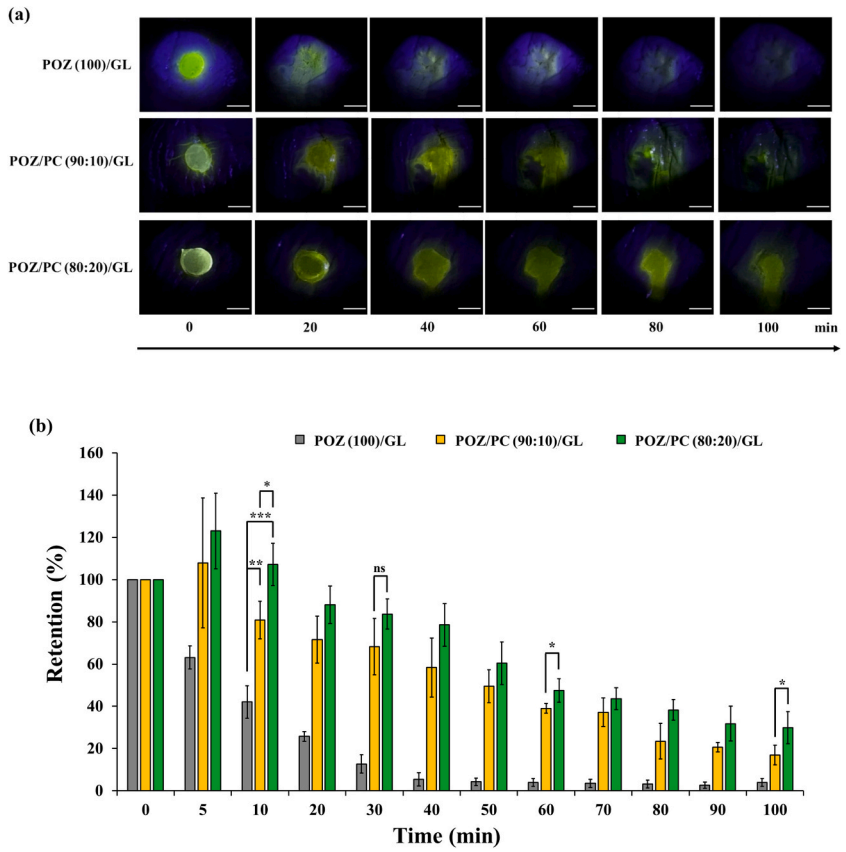

Fig. 7. Mucosal retention of plasticized POZ/GL and POZ/PC/GL films on freshly excised sheep vaginal mucosae after irrigation with different volumes of SVF (100 μL/min) over 100 min: (a) exemplar fluorescent microphotographs. Scale bars are 1 mm; (b) quantitative analysis. All values are the means ± standard deviations of triplicate experiments. Statistically significant differences are given as: * – $p < 0.05$; ** – $p < 0.01$; ***—$p < 0.001$; ns—no significance.

Table 3
Visual and microscopic analysis of polymer films.

Sample	Images of drug-free polymer films	Images of metronidazole – loaded films	Polarized light microscopy images of metronidazole-loaded films
POZ (100) /GL	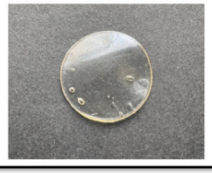	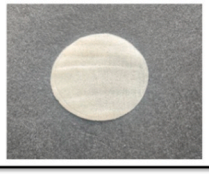	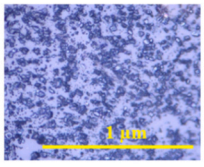
POZ (90:10) /GL		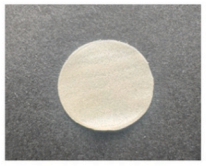	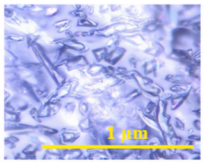
POZ (80:20) /GL		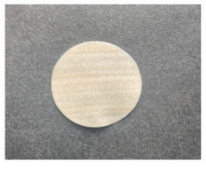	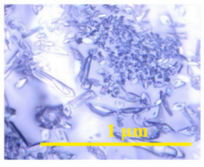

but POZ/PC (80:20)/GL retained around 20 ± 6 % ($p < 0.05$), showing its better resistance to wash-off.

In summary, these retention results suggest that adding PC to POZ improves the films' ability to retain on mucosal surfaces under simulated physiological fluid conditions. This quality is important for vaginal drug delivery systems that need to stay in place for an extended time, allowing for prolonged contact with the tissue and potentially boosting the effectiveness of local treatments. Another important finding is that the retention of the films on mucosal surfaces is not solely determined by their adhesion to the tissue but also depends on their integrity and resistance to dissolution.

3.9. Characterization of Metronidazole-Loaded drug films

The films plasticized with glycerol showed optimal mechanical and mucoadhesive properties and therefore were selected for loading the drug. All three film compositions with and without the drug were visually assessed and their images are presented in Table 3. The drug-free films are transparent, slightly yellowish in color, uniform in weight and thickness, sufficiently elastic, slightly sticky, and without cracks or creases. Metronidazole-loaded films were completely opaque and white, however, not sticky, but also sufficiently elastic, without cracks and creases. The loss of transparency is due to the presence of metronidazole crystals in the polymer film. It is likely that during the extrusion process, drug crystals were uniformly dispersed throughout the polymer matrix. The recrystallization of metronidazole may be partly attributed with its supersaturation within the blend and the presence of glycerol. Junmahasathien et al. [61] similarly reported drug crystallisation specifically in the glycerol-plasticised films.

The images of metronidazole-loaded films were also generated using a polarizing light microscope in reflected light. These images clearly show the presence of the drug crystals uniformly distributed in the polymer matrix. It should be noted that in the POZ/GL (100) film, the crystals appear as a finely dispersed phase, uniformly distributed throughout the matrix. The incorporation of polycarbophil results in the formation of plate-shaped and elongated crystals, and the POZ/PC/GL (80:20) film also exhibiting noticeable crystal accumulation and aggregation. The metronidazole content in these films, as determined by dissolution followed by UV–Vis spectrophotometric analysis, was 38.9 ± 1.4 % w/w. This value is very close to the theoretical loading of 36.7 % w/w. The slight discrepancy between the theoretical and measured drug content may be attributed to residual moisture present in the glycerine and starting polymers.

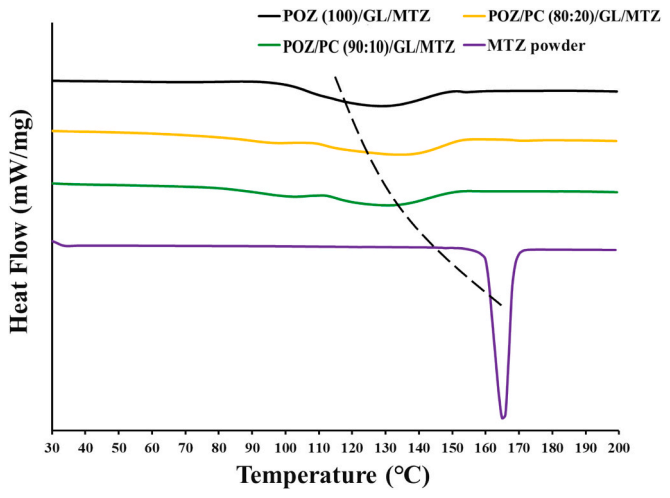

Fig. 8. DSC thermograms of MTZ powder, POZ/MTZ and POZ/PC/MTZ films. Dashed curve shows the trend in endothermic events.

3.10. Evaluation of crystallinity using DSC

The crystallinity of metronidazole in the drug-loaded films was evaluated by DSC, as described in Section 2.3.6. As shown in Fig. 8, the presence of the endothermic melting peaks of metronidazole was observed in all thermograms. Pure MTZ exhibited a distinct sharp melting peak at 165 °C, corresponding to its fully crystalline nature and in good agreement with previously published data [62]. MTZ-loaded films showed a shifted and broadened melting peak with significantly reduced intensity. These thermal changes suggest a partial transition of the drug from a crystalline to an amorphous state within the polymer matrix. Similar behavior was observed by Perioli et al. [63], who reported a decrease in MTZ crystallinity when it was formulated in chitosan/polycarbophil vaginal tablets. In their study, DSC thermograms showed either a reduction or complete disappearance of the drug's melting peak, particularly in the formulations containing greater amounts of polycarbophil, indicating drug–polymer interactions and amorphization. The reduction in the drug crystallinity is supposed to enhance its dissolution, as the amorphous phase generally exhibits increased molecular mobility and higher thermodynamic activity compared to its crystalline counterpart [64].

The degree of MTZ crystallinity in the polymer films was calculated according to Equation (1), based on the specific enthalpy of the melting peak. It was approximately 65 % in the POZ (100) based film, and about 69 % and 70 % in the POZ/PC (90:10) and POZ/PC (80:20) based films, respectively. This observation is consistent with the literature data, which demonstrate partial amorphization of drugs incorporated into hydrophilic polymer carriers [40,41].

Taken together, these results indicate that incorporation of MTZ into POZ/PC films via hot-melt extrusion leads to a partial drug amorphization, which may contribute to its improved dissolution and bioavailability.

3.11. In vitro metronidazole release

Fig. 9 presents data on the in vitro release of metronidazole through a cellulose membrane from polymer films based on POZ/GL and POZ/PC/GL into artificial vaginal fluid. During the first 30–45 min, all tested films released no more than 5 % of metronidazole. This is likely attributed to their dense structure, formed during hot extrusion, which initially limits the diffusion of the drug. However, once the films achieve

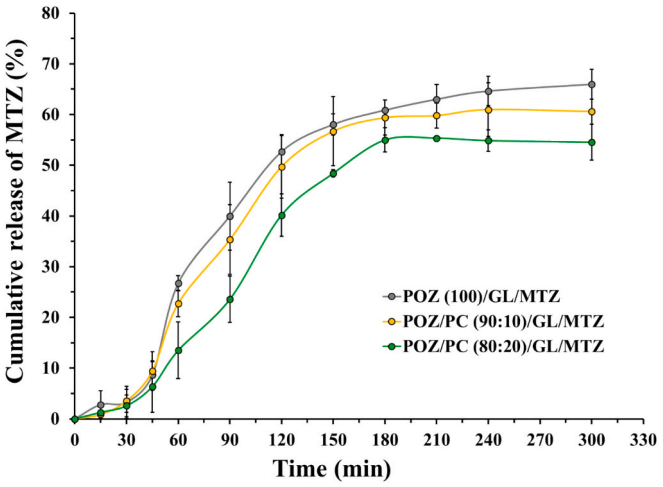

Fig. 9. In vitro cumulative release of metronidazole from POZ/GL and POZ:PC/GL films. Data are presented as mean ± standard deviation (n = 3). Statistical analysis showed no significant difference between POZ(100)/GL/MTZ and POZ/PC(90:10)/GL/MTZ ($p > 0.05$), while a significant difference was observed between POZ(100)/GL/MTZ and POZ/PC(80:20)/GL/MTZ ($p < 0.005$).

better hydration, the release rate of metronidazole increases significantly. By the 6th hour, the cumulative drug release from the POZ/GL film reaches 65.9 ± 2.9 %, while the POZ/PC(90:10)/GL and POZ/PC (80:20)/GL films release 60.6 ± 5.7 % and 54.5 ± 3.5 %, respectively. These results indicate that incorporating PC into the formulation prolongs drug release, with higher PC content producing a more pronounced retardation effect.

The delayed release can be attributed to the weakly cross-linked structure of PC, which may hinder water diffusion into the matrix and restrict the outward diffusion of MTZ. Thus, the incorporation of PC in the film facilitates sustained drug release, which may be advantageous for the development of controlled-release pharmaceutical formulations.

The kinetics of metronidazole release from the films was analyzed using the zero-order, the first-order, the Higuchi, and the Korsmeyer-Peppas models. The results are presented in Table 4 and in Figs. S5-S8 (Supporting information). According to the calculations, the Higuchi model ($R^2 = 0.890 - 0.903$) provides the best fit for the drug release kinetics, indicating a diffusion-controlled mechanism. The addition of polycarbophil (PC) to the formulation leads to a slower release, as evidenced by an increase in the exponent *n* in the Korsmeyer-Peppas model (from 1.221 to 1.426). This suggests that PC forms a denser network, slowing down MTZ diffusion. Thus, the release of metronidazole from the films is diffusion-controlled and depends on the matrix composition, with a higher PC content contributing to a prolonged drug release.

3.12. Antimicrobial studies

The antimicrobial activity of the films containing metronidazole against *Staphylococcus aureus* and *Escherichia coli* was evaluated using the agar disk diffusion method, with the results presented in Fig. 10 and Table 5. Films without active pharmaceutical ingredient showed no inhibition zones against either the Gram-positive or Gram-negative bacterial strains. However, all film samples containing metronidazole exhibited pronounced antimicrobial activity against both *Staphylococcus aureus* and *Escherichia coli*, with inhibition zone diameters being nearly identical for both strains.

Pure metronidazole was used as a control to benchmark the antimicrobial activity of the drug in its free form. To provide a comprehensive assessment, two standard agar diffusion methods were employed: the well diffusion method and the disk diffusion method. These methods were selected to account for possible differences in drug diffusion behaviour between liquid samples and solid films.

In the well diffusion method, circular wells (6 mm in diameter) were created in the agar using a specialised tool, and a defined volume of metronidazole solution was pipetted into each well. This technique enables direct assessment of antimicrobial activity from a liquid formulation.

In contrast, the disk diffusion method was used to more closely mimic the testing conditions applied to the metronidazole-loaded films. In this method, sterile paper disks (6 mm in diameter) were soaked with the drug solution and placed onto the inoculated agar surface, simulating the localized release from a solid matrix.

Interestingly, the inhibition zones observed for pure metronidazole in both methods were smaller than those produced by the metronidazole-loaded films. This difference may be attributed to the presence of glycerol in the film formulations, which could have enhanced the diffusivity of metronidazole within the agar medium. Furthermore, glycerol itself has mild antimicrobial properties, potentially acting synergistically with metronidazole [65].

However, it is important to emphasize that films containing glycerol but no drug did not exhibit any bactericidal effects. Although glycerol may demonstrate weak antimicrobial activity in aqueous solutions [66], its free concentration within the solid polymer matrix is very low and insufficient to inhibit microbial growth. Therefore, the absence of antimicrobial activity in drug-free films confirms the key role of metronidazole in the observed antimicrobial effects.

4. Conclusions

In this study, POZ/PC blend films were developed and comprehensively evaluated for vaginal drug delivery, focusing on achieving an optimal balance of mucoadhesive strength, flexibility, and retention under vaginal fluid flow conditions. The incorporation of PC significantly enhanced the mucoadhesive properties of POZ films, as confirmed through both detachment force measurements and extended retention on mucosal surfaces. The addition of glycerol as a plasticizer further improved films' flexibility and adhesion, with the POZ/PC (80:20)/GL formulation demonstrating the most promising performance in both mucoadhesion and retention tests. *Ex vivo* retention studies revealed that POZ/PC films, particularly those with higher PC content, maintained substantial adhesion even after 100 min of simulated fluid flow, highlighting their potential for applications requiring extended residence on mucosal tissues. These findings indicate that the optimized POZ/PC films prepared via hot-melt extrusion hold strong potential for enhancing vaginal drug delivery systems by promoting prolonged contact with the mucosal surface and facilitating sustained therapeutic effects. However, one important consideration for this approach is the limitation on the proportion of PC that can be incorporated into the blend. While PC imparts desirable mucoadhesive properties, its high viscosity and poor thermoplasticity significantly reduce the extrudability of the formulation during hot-melt processing. In this study, we found that incorporating PC at levels above 20 % leads to processing challenges, such as poor flowability and difficulties in forming uniform films. Therefore, although the POZ/PC blends offer a promising platform for vaginal drug delivery, the proportion of PC in the formulation must be carefully optimized to balance mucoadhesion, processability, and mechanical integrity of the final dosage form.

DSC analysis confirmed partial amorphization of metronidazole within the POZ/PC matrix, reducing its crystallinity from 100 % in the pure drug to approximately 65–70 % in the films. This change in solid-state characteristics likely contributes to the improved dissolution behavior of metronidazole. Furthermore, the drug-loaded films exhibited significant antimicrobial activity against both *Staphylococcus aureus* and *Escherichia coli* in standard agar diffusion assays. These results underscore the dual benefits of structural modification and polymer-based formulation in enhancing the local therapeutic efficacy of poorly soluble antimicrobial agents.

Table 4
Kinetic data from *in vitro* release studies for metronidazole topical formulations.

Film formulation	Zero order		First order		Higuchi's model		Korsmeyer-Peppas's model	
	Release rate constant (K_0)	R^2	Release rate constant (K_1)	R^2	Release rate constant (K_H)	R^2	Release rate constant (n)	R^2
POZ(100)/GL/MTZ	0.259	0.848	$2{\cdot}10^{-85}$	0.895	4.988	0.903	1.221	0.894
POZ/PC(90:10)/GL/MTZ	0.246	0.840	$2{\cdot}10^{-5}$	0.841	4.746	0.897	1.426	0.901
POZ/PC(80:20)/GL/MTZ	0.230	0.873	$2{\cdot}10^{-5}$	0.874	4.351	0.890	1.398	0.946

Note: R^2 = coefficient of linear regression.

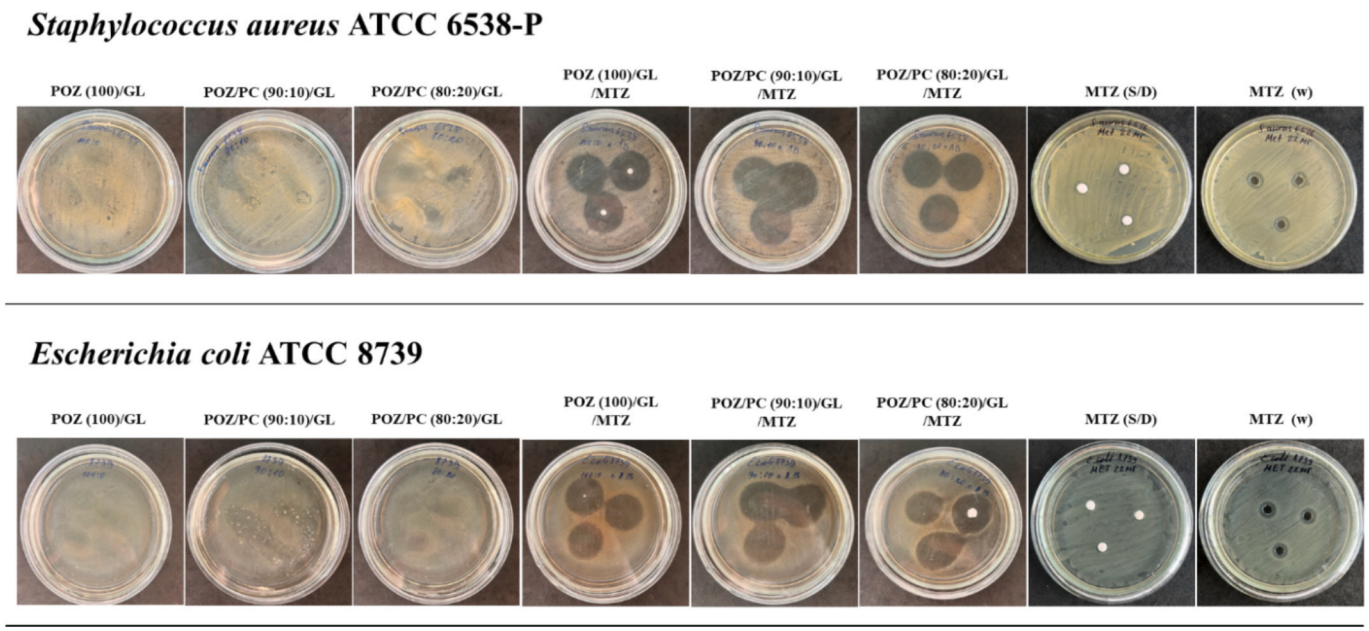

Fig. 10. Results of antimicrobial activity of polymeric films against Gram-positive *Staphylococcus aureus* ATCC 6538-P and Gram-negative *Escherichia coli* bacteria ATCC 8739.

Table 5
Bacteria growth inhibition zones in the presence of the drug-loaded polymeric films and controls.

Film formulation	Diameter of Growth Inhibition Zone (mm)	
	Staphylococcus aureus	*Escherichia coli*
Drug-Free Films		
POZ (100)/GL	0	0
POZ/PC(90:10)/GL	0	0
POZ/PC(80:20)/GL	0	0
Drug-Loaded Films		
POZ (100)/GL/MTZ	28.00 ± 0.00	28.33 ± 2.88
POZ/PC(90:10)/GL/MTZ	33.33 ± 1.15	29.33 ± 1.15
POZ/PC(80:20)/GL/MTZ	30.00 ± 0.00	30.00 ± 0.00
Control Sample		
MTZ (w)	12.33 ± 0.58	10.00 ± 0.00
MTZ (S/D)	7.33 ± 0.58	7.00 ± 0.00

Note: S/D – sterile discs; w – well diffusion method; ∅ = 6 mm (diameter of the disc/well).

5. Author statement

All authors have read and approved the final version of the manuscript. We confirm that the work described is original, has not been published previously, and is not under consideration for publication elsewhere. All authors have made substantial contributions to the conception, design, execution, and/or interpretation of the study. There are no known conflicts of interest associated with this publication, and there has been no significant financial support for this work that could have influenced its outcome. The authors agree to comply with the ethical standards and editorial policies of the European Polymer Journal.

Declaration of generative AI and AI-assisted technologies in the writing process

During the preparation of this work the author(s) used ChatGPT (OpenAI) to assist with the clarity and flow of some parts of the manuscript. After using this tool/service, the author(s) reviewed and edited the content as needed and take(s) full responsibility for the content of the publication.

CRediT authorship contribution statement

Marzhan K. Akhmetova: Writing – original draft, Methodology, Investigation, Formal analysis. **Guzel K. Abilova:** Writing – original draft, Project administration, Methodology, Investigation, Formal analysis. **Aknaz B. Duisengali:** Investigation. **Tomiris A. Nurlybaeva:** Investigation. **Sanimai S. Uzakbaeva:** Investigation. **Galiya S. Irmukhametova:** Supervision, Resources. **Amirbek Z. Bekeshev:** Supervision, Resources. **Vitaliy V. Khutoryanskiy:** Writing – review & editing, Supervision, Resources, Conceptualization.

Declaration of competing interest

The authors declare the following financial interests/personal relationships which may be considered as potential competing interests: Guzel K. Abilova reports financial support was provided by The Science Committee of the Ministry of Science and Higher Education of the Republic of Kazakhstan. Marzhan K. Akhmetova reports financial support was provided by The Science Committee of the Ministry of Science and Higher Education of the Republic of Kazakhstan. Vitaliy V. Khutoryanskiy reports financial support was provided by The Royal Society. If there are other authors, they declare that they have no known competing financial interests or personal relationships that could have appeared to influence the work reported in this paper.

Acknowledgements

G.K.A. would like to thank the Science Committee of the Ministry of Science and Higher Education of the Republic of Kazakhstan for the research grant for young scientists «Zhas Galym» No. AP15473201. The authors would like to thank Arbuz Alexander (Nazarbayev University, Astana, Kazakhstan) for assistance in scanning electron microscopy experiments and Daulet Kaldybekov (Al-Farabi Kazakh National University, Almaty, Kazakhstan) for FTIR spectroscopy experiments. The authors also wish to express their sincere gratitude to Ardak Dzhumagazieva, Head of the Microbiology Laboratory, and Zhanar Iskakbaeva, Deputy Head of the Microbiology Laboratory, at JSC "Scientific Center

for Anti-Infective Drugs" (Almaty, Kazakhstan) for their invaluable contributions to the antimicrobial activity studies of the film samples. V. V.K. acknowledges the Royal Society for funding his industry fellowship (IF/R2/222031).

Appendix A. Supplementary material

Supplementary data to this article can be found online at https://doi.org/10.1016/j.eurpolymj.2025.114175.

Data availability

Data will be made available on request.

References

[1] J. Das Neves, M.H. Amaral, M.F. Bahia, Vaginal Drug delivery, in, Pharm. Sci. Encycl. Drug Discov. Dev. Manuf. (2010) 809–878, https://doi.org/10.1002/9780470259818.ch22.
[2] P.Y. Ziyi Yang, Xueqing Wu, Hongmin Wang, Jie Zhou, Xia Lin, Vagina, a promising route for drug delivery, J. Drug Deliv. Sci. Technol. 93 (2024) 105397. Doi: Doi: 10.1016/j.jddst.2024.105397.
[3] C.K. Sahoo, P. Kumar Nayak, D.K. Sarangi, T.K. Sahoo, Intra Vaginal Drug delivery system: an overview, Am. J. Adv. Drug Deliv. 1 (2013) 43–45, http://doi.org/ISSN-2321-547X.
[4] R. Noor-ul-ain, N. Ilyas, M. Saeed, G. Subramaniam, A. Mastinu, Industrial Crops & Products Advances in pharmaceutical and biomedical applications of plant – based nano-biopolymers with special emphasis on vaginal drug delivery systems : a review, Ind. Crop Prod. 225 (2025) 120592, https://doi.org/10.1016/j.indcrop.2025.120592.
[5] N.R. Naveen, C. Gopinath, D.S. Rao, A spotlight on thiolated natural polymers and their relevance in mucoadhesive drug delivery system, Futur, J. Pharm. Sci. 4 (2018) 47–52, https://doi.org/10.1016/j.fjps.2017.08.002.
[6] Y.H. Dinakar, Mucoadhesive means of drug delivery – an appraise, ARC J. Pharm. Sci. 4 (2018) 21–28, https://doi.org/10.20431/2455-1538.0403004.
[7] V.V. Khutoryanskiy, Advances in Mucoadhesion and Mucoadhesive Polymers, Macromol. Biosci. 11 (2011) 748–764, https://doi.org/10.1002/mabi.201000388.
[8] K.S. Yadav, G. Soni, D. Choudhary, A. Khanduri, A. Bhandari, G. Joshi, Microemulsions for enhancing drug delivery of hydrophilic drugs : Exploring various routes of administration, Med. Drug Discov. 20 (2023) 100162, https://doi.org/10.1016/j.medidd.2023.100162.
[9] R. Shaikh, T. Raghu, R. Singh, M.J. Garland, A. David, R.F. Donnelly, Mucoadhesive drug delivery systems, J. Pharm. Bioallied Sci. 3 (2011) 89–100, https://doi.org/10.4103/0975-7406.76478.
[10] M. Edman, K. Lindell, D. Topgaard, Q. Dat, N. Sofi, M. Wahlgren, Mucoadhesion: mucin-polymer molecular interactions, Int. J. Pharm. 610 (2021) 121245, https://doi.org/10.1016/j.ijpharm.2021.121245.
[11] M.S. Lalan, V.N. Patel, A. Misra, Polymers in Vaginal Drug delivery: recent Advancements, Inc (2020), https://doi.org/10.1016/B978-0-12-819659-5.00010-0.
[12] M.T.M. Subi, N. Selvasudha, H.R. Vasanthi, Vaginal drug delivery system : a promising route of drug administration for local and systemic diseases, Drug Discov. Today 29 (2024) 104012, https://doi.org/10.1016/j.drudis.2024.104012.
[13] T. Osmałek, A. Froelich, B. Jadach, A. Tatarek, P. Gadzi, M. Ekert, V. Puri, J. Wroty, Recent advances in Polymer-based Vaginal Drug delivery Systems, Pharmaceutics 13 (2021) 1–49.
[14] C.M. Caramella, S. Rossi, F. Ferrari, M.C. Bonferoni, G. Sandri, Mucoadhesive and thermogelling systems for vaginal drug delivery, Adv. Drug Deliv. Rev. 92 (2015) 39–52, https://doi.org/10.1016/j.addr.2015.02.001.
[15] M. Hernández-González, C. Rodríguez-González, M. Domínguez-Acosta, J. Hernández-Paz, I. Olivas-Armendáriz, Mucoadhesive polymeric systems for vaginal drug delivery: a systemic review, Rev. Mex. Ing. Biomed. 44 (2023) 38–51, https://doi.org/10.17488/RMIB.44.2.4.
[16] R.R. De Araújo Pereira, M.L. Bruschi, Vaginal mucoadhesive drug delivery systems, drug Dev, Ind. Pharm. 38 (2012) 643–652, https://doi.org/10.3109/03639045.2011.623355.
[17] F. Acarturk, Mucoadhesive Vaginal Drug delivery Systems, Recent Pat. Drug Deliv. Formul. 3 (2009) 193–205, https://doi.org/10.2174/187221109789105658.
[18] E. Pacheco-quito, L. Bedoya, J. Rubio, A. Tamayo, R. Ruiz-caro, M. Veiga, Layer-by-layer vaginal films for acyclovir controlled release to prevent genital herpes, Int. J. Pharm. 627 (2022) 122239, https://doi.org/10.1016/j.ijpharm.2022.122239.
[19] A. Martín-illana, E. Chinarro, R. Cazorla-luna, F. Notario-perez, D. Veiga-ochoa, J. Rubio, A. Tamayo, Optimized hydration dynamics in mucoadhesive xanthan-based trilayer vaginal films for the controlled release of tenofovir, Carbohydr. Polym. 278 (2022) 118958, https://doi.org/10.1016/j.carbpol.2021.118958.
[20] F. Notario-pérez, R. Cazorla-luna, A. Martín-illana, J. Galante, R. Ruiz-caro, J. Neves, M. Veiga, Design , fabrication and characterisation of drug-loaded vaginal films : State, J. Control. Release 327 (2020) 477–499, https://doi.org/10.1016/j.jconrel.2020.08.032.
[21] J. Conte, R. Henrique, M. Paludetto, R. Monte, I. Fabrícia, A. Luis, T. Caon, Development of biopolymer films loaded with fluconazole and thymol for resistant vaginal candidiasis, Int. J. Biol. Macromol. 275 (2024) 133356, https://doi.org/10.1016/j.ijbiomac.2024.133356.
[22] N.L. Calvo, L.A. Svetaz, V.A. Alvarez, A.D. Quiroga, M.C. Lamas, D. Leonardi, Chitosan-hydroxypropyl methylcellulose tioconazole films: a promising alternative dosage form for the treatment of vaginal candidiasis, Int. J. Pharm. 556 (2019) 181–191, https://doi.org/10.1016/j.ijpharm.2018.12.011.
[23] M.L. Gerton, B.K. Mann, Mucoadhesive hyaluronic acid-based films for vaginal delivery of metronidazole, J. Biomed. Mater. Res. - Part B Appl. Biomater. 109 (2021) 1706–1712, https://doi.org/10.1002/jbm.b.34827.
[24] A. Villar-padilla, M.L. Del Prado-audelo, M. González-torres, D.M. Giraldo-gomez, I.H. Caballero-florán, M.G. Carmen, J. Sharifi-rad, G. Figueroa-gonzález, Development of a xanthan gum film for the possible treatment of vaginal infections, Cell. Mol. Biol. 67 (2021) 80–88, https://doi.org/10.14715/cmb/2021.67.1.12.
[25] S. Karki, H. Kim, S.J. Na, D. Shin, K. Jo, J. Lee, Thin films as an emerging platform for drug delivery, Asian J. Pharm. Sci. 11 (2016) 559–574, https://doi.org/10.1016/j.ajps.2016.05.004.
[26] F.V. Borbolla-jim, S.I. Peña-corona, S.J. Farah, E. Pineda-p, A. Romero-montero, S. Alberto, J.J. Magaña, G. Leyva-g, Films for wound healing fabricated using a solvent casting technique, Pharmaceutics 15 (2023) 1–27.
[27] D.A. Miller, J.T. Mcconville, W.E.I. Yang, R.O.W. Iii, J.W. Mcginity, Hot-Melt extrusion for enhanced delivery of drug particles, J. Pharceutical Sci. 96 (2007) 361–376, https://doi.org/10.1002/jps.
[28] M.F. Simões, R.M.A. Pinto, S. Simões, Hot-melt extrusion in the pharmaceutical industry: toward filing a new drug application, Drug Discov. Today 24 (2019) 1749–1768, https://doi.org/10.1016/j.drudis.2019.05.013.
[29] J. Breitenbach, Melt extrusion: from process to drug delivery technology, Eur. J. Pharm. Biopharm. 54 (2002) 107–117, https://doi.org/10.1016/S0939-6411(02)00061-9.
[30] C. De Brabander, C. Vervaet, L. Van Bortel, J.P. Remon, Bioavailability of ibuprofen from hot-melt extruded mini-matrices, Int. J. Pharm. 271 (2004) 77–84, https://doi.org/10.1016/j.ijpharm.2003.10.029.
[31] M.A. Repka, K. Gutta, S. Prodduturi, M. Munjal, S.P. Stodghill, Characterization of cellulosic hot-melt extruded films containing lidocaine, Eur. J. Pharm. Biopharm. 59 (2005) 189–196, https://doi.org/10.1016/j.ejpb.2004.06.008.
[32] Z. Zhang, S. Feng, R. El-kanayati, I. Karnik, Novel development of Poly (2-ethyl-2-oxazoline) -based mucoadhesive buccal film for poorly water-soluble drug delivery via hot-melt extrusion, Eur. J. Pharm. Biopharm. 210 (2025) 114686, https://doi.org/10.1016/j.ejpb.2025.114686.
[33] B. Claeys, A. Vervaeck, C. Vervaet, J.P. Remon, R. Hoogenboom, B.G. De Geest, Poly (2-ethyl-2-oxazoline) as Matrix Excipient for Drug Formulation by Hot Melt Extrusion and Injection Molding, Macromol. Rapid Commun. 33 (2012) 1701–1707, https://doi.org/10.1002/marc.201200332.
[34] A. Samaro, M. Vergaelen, M. Purino, A. Tigrine, V.R. De, N. Moazami, M.N. Boone, R. Hoogenboom, C. Vervaet, Poly (2-alkyl-2-oxazoline)s: a polymer platform to sustain the release from tablets with a high drug loading, Mater. Today Bio 16 (2022) 100414, https://doi.org/10.1016/j.mtbio.2022.100414.
[35] T. Lorson, M.M. Lübtow, E. Wegener, M.S. Haider, S. Borova, D. Nahm, R. Jordan, M. Sokolski-papkov, A.V. Kabanov, R. Luxenhofer, Biomaterials Poly (2-oxazoline) s based biomaterials : a comprehensive and critical update, Biomaterials 178 (2018) 204–280, https://doi.org/10.1016/j.biomaterials.2018.05.022.
[36] R. Hoogenboom, H. Schlaad, Thermoresponsive poly(2-oxazoline)s, polypeptoids, and polypeptides, Polym. Chem. 8 (2017) 24–40, https://doi.org/10.1039/c6py01320a.
[37] M.A. Repka, J.W. McGinity, Bioadhesive properties of hydroxypropylcellulose topical films produced by hot-melt extrusion, J. Control. Release 70 (2001) 341–351, https://doi.org/10.1016/S0168-3659(00)00365-5.
[38] M.A. Repka, J.W. McGinity, Physical-mechanical, moisture absorption and bioadhesive properties of hydroxypropylcellulose hot-melt extruded films, Biomaterials 21 (2000) 1509–1517, https://doi.org/10.1016/S0142-9612(00)00046-6.
[39] S.B. De Souza Ferreira, J.B. Da Silva, F.B. Borghi-Pangoni, M.V. Junqueira, M. L. Bruschi, Linear correlation between rheological, mechanical and mucoadhesive properties of polycarbophil polymer blends for biomedical applications, J. Mech. Behav. Biomed. Mater. 68 (2017) 265–275, https://doi.org/10.1016/j.jmbbm.2017.02.016.
[40] X. Shan, M.A. Moghul, A.C. Williams, V.V. Khutoryanskiy, Mutual Effects of hydrogen bonding and polymer hydrophobicity on ibuprofen crystal inhibition in solid dispersions with poly (N -vinyl pyrrolidone) and poly (2-oxazolines), Pharmaceutics 13 (5) (2021).
[41] X. Shan, A.C. Williams, V.V. Khutoryanskiy, Polymer structure and property effects on solid dispersions with haloperidol : Poly (N-vinyl pyrrolidone) and poly (2-oxazolines) studies, Int. J. Pharm. 590 (2020) 119884.
[42] G.K. Abilova, S.F. Nasibullin, K. Ilyassov, A.N. Adilov, M.K. Akhmetova, R. I. Moustafine, Y.T. Muratov, S.E. Kudaibergenov, V.V. Khutoryanskiy, Mucoadhesive gellan gum / poly (2-ethyl-2-oxazoline) films for ocular delivery of pilocarpine hydrochloride, J. Drug Deliv. Sci. Technol. 104 (2025) 106492, https://doi.org/10.1016/j.jddst.2024.106492.
[43] E.O. Shatabayeva, D.B. Kaldybekov, Z.A. Kenessova, R.N. Tuleyeva, Development of mucoadhesive vaginal films for metronidazole delivery using methacryloylated , crotonoylated , and itaconoylated gelatin blends with poly (vinyl alcohol, AAPS PharmSciTech 26 (2025) 63, https://doi.org/10.1208/s12249-025-03055-1.
[44] M.A. Repka, T.G. Gerding, S.L. Repka, J.W. McGinity, Influence of plasticizers and drugs on the physical-mechanical properties of hydroxypropylcellulose films prepared by hot melt extrusion, Drug Dev. Ind. Pharm. 25 (1999) 625–633, https://doi.org/10.1081/DDC-100102218.

[45] G.K. Abilova, D.B. Kaldybekov, G.S. Irmukhametova, D.S. Kazybayeva, Z. A. Iskakbayeva, S.E. Kudaibergenov, V.V. Khutoryanskiy, Chitosan/Poly(2-ethyl-2-oxazoline) Films with Ciprofloxacin for Application in Vaginal Drug delivery, Materials (basel). 13 (2020) 1709, https://doi.org/10.3390/ma13071709.
[46] L. Phuong Ta, E. Bujna, S. Kun, D. Charalampopoulos, V.V. Khutoryanskiy, Electrosprayed mucoadhesive alginate-chitosan microcapsules for gastrointestinal delivery of probiotics, Int. J. Pharm. 597 (2021) 120342, https://doi.org/10.1016/j.ijpharm.2021.120342.
[47] E.O. Shatabayeva, D.B. Kaldybekov, L. Ulmanova, B.A. Zhaisanbayeva, E.A. Mun, Z.A. Kenessova, S.E. Kudaibergenov, V.V. Khutoryanskiy, Enhancing mucoadhesive properties of gelatin through chemical modification with unsaturated anhydrides, Biomacromolecules 25 (2024) 1612–1628, https://doi.org/10.1021/acs.biomac.3c01183.
[48] M. Balouiri, M. Sadiki, S.K. Ibnsouda, Methods for in vitro evaluating antimicrobial activity : a review, J. Pharm. Anal. 6 (2016) 71–79, https://doi.org/10.1016/j.jpha.2015.11.005.
[49] H. Abdelkader, B. Pierscionek, R.G. Alany, Novel in situ gelling ocular films for the opioid growth factor-receptor antagonist-naltrexone hydrochloride: Fabrication, mechanical properties, mucoadhesion, tolerability and stability studies, Int. J. Pharm. 477 (2014) 631–642, https://doi.org/10.1016/j.ijpharm.2014.10.069.
[50] M. Tighsazzadeh, J.C. Mitchell, J.S. Boateng, Development and evaluation of performance characteristics of timolol-loaded composite ocular films as potential delivery platforms for treatment of glaucoma, Int. J. Pharm. 566 (2019) 111–125, https://doi.org/10.1016/j.ijpharm.2019.05.059.
[51] G.K. Abilova, D.B. Kaldybekov, E.K. Ozhmukhametova, A.Z. Saimova, D. S. Kazybayeva, G.S. Irmukhametova, V.V. Khutoryanskiy, Chitosan/poly(2-ethyl-2-oxazoline) films for ocular drug delivery: Formulation, miscibility, in vitro and in vivo studies, Eur. Polym. J. 116 (2019) 311–320, https://doi.org/10.1016/j.eurpolymj.2019.04.016.
[52] R.I. Moustafine, A.S. Viktorova, V.V. Khutoryanskiy, Interpolymer complexes of carbopol® 971 and poly(2-ethyl-2-oxazoline): Physicochemical studies of complexation and formulations for oral drug delivery, Int. J. Pharm. 558 (2019) 53–62, https://doi.org/10.1016/j.ijpharm.2019.01.002.
[53] J. Lavikainen, M. Dauletbekova, G. Toleutay, M. Kaliva, M. Chatzinikolaidou, S. E. Kudaibergenov, A. Tenkovtsev, V.V. Khutoryanskiy, M. Vamvakaki, V. Aseyev, Poly (2-ethyl-2-oxazoline) grafted gellan gum for potential application in transmucosal drug delivery, Polym. Adv. Technol. 32 (2021) 2770–2780, https://doi.org/10.1002/pat.5298.
[54] S. Baldassari, P. Cirrincione, G. Ailuno, G. Drava, S. Arpicco, G. Caviglioli, Towards a better understanding of thermally treated polycarbophil matrix tablets for controlled release, Int. J. Pharm. X 3 (2021) 100098, https://doi.org/10.1016/j.ijpx.2021.100098.
[55] G. Caviglioli, S. Baldassari, P. Cirrincione, E. Russo, B. Parodi, P. Gatti, G. Drava, An innovative matrix controlling drug delivery produced by thermal treatment of DC tablets containing polycarbophil and ethylcellulose, Int. J. Pharm. 458 (2013) 74–82, https://doi.org/10.1016/j.ijpharm.2013.10.014.
[56] C. Guo, Y. Han, W. Zhao, X. Zhang, Adsorption properties for ammonia nitrogen by polyacrylic acid / sodium alginate-based titanium dioxide composite hydrogel, Desalin. Water Treat. 316 (2023) 383–394, https://doi.org/10.5004/dwt.2023.30208.
[57] S. Soradech, P. Kengkwasingh, A.C. Williams, V.V. Khutoryanskiy, Synthesis and Evaluation of Poly(3-hydroxypropyl Ethylene-imine) and its Blends with Chitosan Forming Novel Elastic Films for delivery of Haloperidol, Pharmaceutics 14 (2022) 2671, https://doi.org/10.3390/pharmaceutics14122671.
[58] N. Hernandez-Montero, J.M. Ugartemendia, H. Amestoy, J.R. Sarasua, Complex phase behavior and state of miscibility in poly(ethylene glycol)/poly(l -lactide-co-ε-caprolactone) blends, J. Polym. Sci., Part B: Polym. Phys. 52 (2014) 111–121, https://doi.org/10.1002/polb.23394.
[59] P. Paolicelli, S. Petralito, G. Varani, M. Nardoni, S. Pacelli, L. Di Muzio, J. Tirillò, C. Bartuli, S. Cesa, M.A. Casadei, A. Adrover, Effect of glycerol on the physical and mechanical properties of thin gellan gum films for oral drug delivery, 2018. Doi: 10.1016/j.ijpharm.2018.05.046.
[60] R.P. Kambour, J.M. Kelly, B.J. McKinley, Modulus and yield resistance of glassy blends containing diluents manifesting varying degrees of mobility: polyphenylene ether/polystyrene/diluent mixtures, J. Polym. Sci., Part B: Polym. Phys. 27 (1989) 1979–1992, https://doi.org/10.1002/polb.1989.090271003.
[61] T. Junmahasathien, P. Panraksa, P. Protiarn, D. Hormdee, Preparation and evaluation of metronidazole-loaded pectin films for potentially targeting a microbial infection associated with periodontal disease, Polymers (basel). 10 (2018) 1021, https://doi.org/10.3390/polym10091021.
[62] M. Ghavami-lahiji, F. Sha, F. Naja, M. Erfan, Drug-loaded polymeric fi lms as a promising tool for the treatment of periodontitis, J. Drug Deliv. Sci. Technol. 52 (2019) 122–129, https://doi.org/10.1016/j.jddst.2019.04.034.
[63] L. Perioli, V. Ambrogi, C. Pagano, S. Scuota, C. Rossi, FG90 chitosan as a new polymer for metronidazole mucoadhesive tablets for vaginal administration, Int. J. Pharm. 377 (2009) 120–127, https://doi.org/10.1016/j.ijpharm.2009.05.016.
[64] D.U. Kapoor, S. Singh, P. Sharma, B.G. Prajapati, Amorphization of low soluble drug with amino acids to improve its therapeutic efficacy: a state - of - art - review, AAPS PharmSciTech 24 (2023) 1–30, https://doi.org/10.1208/s12249-023-02709-2, 253.
[65] T.M. Nalawade, K. Bhat, S.H.P. Sogi, Bactericidal activity of propylene glycol, glycerine, polyethylene glycol 400, and polyethylene glycol 1000 against selected microorganisms, J. Int. Soc. Prev. Community Dent. 5 (2015) 114–119, https://doi.org/10.4103/2231-0762.155736.
[66] A.S. Sleem, S.S. Salman, W.A. Shehata, A.M. Dawoud, Evaluation of glycerol antiseptic effect on gram positive and gram negative bacteria, Menoufia Med. J. 36 (2023) 9.